

J A E R I - M
93-012

NEUTRON TRANSMISSION MEASUREMENTS ON
 ^{121}Sb , ^{123}Sb , ^{140}Ce AND ^{142}Ce
IN THE RESONANCE REGION

February 1993

Makio OHKUBO, Motoharu MIZUMOTO
and Yutaka NAKAJIMA

JAERI-Mレポートは、日本原子力研究所が不定期に公刊している研究報告書です。

入手の問合わせは、日本原子力研究所技術情報部情報資料課（〒319-11 茨城県那珂郡東海村）あて、お申しこみください。なお、このほかに財団法人原子力弘済会資料センター（〒319-11 茨城県那珂郡東海村日本原子力研究所内）で複写による実費領布をおこなっております。

JAERI-M reports are issued irregularly.

Inquiries about availability of the reports should be addressed to Information Division Department of Technical Information, Japan Atomic Energy Research Institute, Tokaimura, Naka-gun, Ibaraki-ken 319-11, Japan.

© Japan Atomic Energy Research Institute, 1993

編集兼発行 日本原子力研究所
印 刷 ニッセイエプロ株式会社

Neutron Transmission Measurements on
 ^{121}Sb , ^{123}Sb , ^{140}Ce and ^{142}Ce
in the Resonance Region

Makio OHKUBO, Motoharu MIZUMOTO and Yutaka NAKAJIMA

Department of Physics
Tokai Research Establishment
Japan Atomic Energy Research Institute
Tokai-mura, Naka-gun, Ibaraki-ken

(Received January 8, 1993)

Neutron transmission measurements have been made on natural antimony, natural cerium, separated isotopes Sb-121, Sb-123, and Ce-142 at the TOF facility of the Japan Atomic Energy Research Institute linear accelerator. Resonance parameters are determined on many levels of Sb-121 and Sb-123 up to 5.3 keV, and Ce-140 and Ce-142 up to 50 keV. S-wave strength function S_0 , and average s-wave level spacing D were deduced as follows:

^{121}Sb :	$S_0 = (0.24 \pm 0.03) \times 10^{-4}$	for 188 levels below 5.3 keV
	$D = 10.3 \pm 0.5$ eV	$E < 0.6$ keV
^{123}Sb :	$S_0 = (0.25 \pm 0.03) \times 10^{-4}$	for 202 levels below 5.3 keV
	$D = 20 \pm 1$ eV	$E < 1.3$ keV
^{140}Ce :	$S_0 = (1.6 \pm 0.5) \times 10^{-4}$	for 15 levels below 50 keV
	$D = 3.5 \pm 0.8$ keV	$E < 50$ keV
^{142}Ce :	$S_0 = (2.7 \pm 0.6) \times 10^{-4}$	for 38 levels below 50 keV
	$D = 2.3 \pm 0.2$ keV	$E < 10$ keV

Keywords: Neutron Cross Sections, Time-of-flight, Transmission Measurements, $^{121,123}\text{Sb}$, $^{140,142}\text{Ce}$, Strength Functions
Average Level Spacings, Resonance Parameters

共鳴領域における¹²¹Sb, ¹²³Sb, ¹⁴⁰Ce, ¹⁴²Ce の中性子透過率測定

日本原子力研究所東海研究所物理部
大久保牧夫・水本 元治・中島 豊

(1993年1月8日受理)

原研リニアックの飛行時間測定装置を用いて、天然アンチモン、天然セリウム、分離アイソトープ Sb-121, Sb-123 及び Ce-142 の中性子透過率を測定した。Sb-121, 123 については 5.3 keV まで、Ce-140, 142 については 50 keV までの多数の共鳴パラメータを得た。S 波強度関数 S_0 、平均準位間隔 D につき以下の値を得た。

$$^{121}\text{Sb} : S_0 = (0.24 \pm 0.03) \times 10^{-4}$$

$$D = 10.3 \pm 0.5 \text{ eV}$$

$$^{123}\text{Sb} : S_0 = (0.25 \pm 0.03) \times 10^{-4}$$

$$D = 20 \pm 1 \text{ eV}$$

$$^{140}\text{Ce} : S_0 = (1.6 \pm 0.5) \times 10^{-4}$$

$$D = 3.5 \pm 0.8 \text{ keV}$$

$$^{142}\text{Ce} : S_0 = (2.7 \pm 0.6) \times 10^{-4}$$

$$D = 2.3 \pm 0.2 \text{ keV}$$

Contents

1. Introduction	1
2. Measurements and Analyses	2
3. Results of Analyses	4
3.1 Antimony	4
3.2 Cerium	5
4. Discussions	7
Acknowledgments	8
References	9

目 次

1. はじめに	1
2. 測定と解析	2
3. 解析結果	4
3.1 アンチモン	4
3.2 セリウム	5
4. 議論	7
謝辞	8
参考文献	9

1. Introduction

Neutron cross section measurements have been continued for more than four decades with a strong demand from reactor technology. In the low energy region, neutron cross sections for medium and heavy nuclei are characterized by fine structure resonances. It is quite well established that average cross sections and average resonance parameters are described by optical model, and distribution laws of level spacings and that of widths by random matrix theories.

However, there are experimental evidences which show deviation from those predictions. One example is existence of intermediate structures; enhancement of resonance strength in the certain energy region. These intermediate structures are often reported in light nuclei as well as in the vicinity of neutron magic nuclei. In ^{140}Ce (N=82) and its neighbouring nuclei, intermediate structures are reported.^{1,2)} So it is interesting to measure the resonances in ^{140}Ce and ^{142}Ce in wide energy region.

Another example is properties of resonance level dispositions, which seems to show a regular level sequence. These sequential level structures are observed in the variety of nuclei; a typical simple sequence in ^{123}Sb was reported previously³⁾. These two features seem to be interrelated with each other; the resonance levels look like to dispose around large resonances with regular level spacings. It is one of the interesting problem how to explain structures of highly excited nuclear states.

For these reasons we measured the resonance parameters on antimony (Z=51) and cerium(Z=58).

The major previous data on antimony resonances are as follows: Wynchank et al.⁴⁾ of Columbia University reported in 1968 the resonance parameters of natural antimony up to 3 keV by the transmission measurements. Muradyan et al.⁵⁾ of Kurchatov Institute reported in 1968 the resonance parameters of ^{121}Sb up to 2.5 keV, and ^{123}Sb up to 4.1 keV by transmission and capture measurements on separated isotopes. The present authors made transmission measurements on natural antimony up to 1.4 keV in 1975⁶⁾. At that time it was reported that in many nuclei including

^{123}Sb , the resonance levels prefer equidistant dispositions with unit spacing of 5.5 or 11 eV or its integer multiples.³⁾

The previous data on cerium are as follows: The neutron transmission measurements on ^{140}Ce have been made by Camarda to 240 keV,¹⁾ and the capture measurements by Musgrove et al. to 63 keV.⁷⁾ On the other hand, the resonance parameters of ^{142}Ce are poorly known, although measurements were made by Newson et al. in 1959,⁸⁾ and Vertebny et al. in 1970.⁹⁾ Cerium isotopes situate at a steep slope of the 4s peak of s-wave strength function. In addition, ^{140}Ce is a neutron magic nucleus($N=82$). For the applied purpose, cerium is included in the ^6Li -glass neutron scintillator as an activator(atomic ratio $\sim 10^{-3}$), so its cross section, especially at an 1.2 keV resonance region, is important for accurate efficiency calculations. Also cerium isotopes are fission product nuclei, their cross sections are related to reactor design.

We have made a series of transmission and capture measurements using a TOF facility of the JAERI linac, on many elements including separated isotope samples during period from 1982 to 1986. Resonance parameters and total cross sections deduced have been sent to NEA DATA BANK, and are compiled in a reference data book, "Neutron Cross Sections", Vol 1¹⁰⁾ and Vol 2¹¹⁾. A part of work on antimony was reported in a progress report,¹²⁾ and that on cerium was already published in the proceedings of the Int. Conf. on Nuclear Data, held at Santa Fe in 1985.¹³⁾

2. Measurements and Analyses

Transmission measurements were carried out at a 47-m TOF station of the JAERI electron linac,^{14,15)} a bird's eye view of which is shown in Fig.1. The linac produced pulsed electron beam of which energy was 120 MeV, peak current $\sim 3\text{A}$, pulse width 25ns and repetition rate 600 pps. Neutrons were produced at a water cooled tantalum target bombarded by the electron beam, and were moderated by a surrounding moderator. The target-moderator system

^{123}Sb , the resonance levels prefer equidistant dispositions with unit spacing of 5.5 or 11 eV or its integer multiples.³⁾

The previous data on cerium are as follows: The neutron transmission measurements on ^{140}Ce have been made by Camarda to 240 keV,¹⁾ and the capture measurements by Musgrove et al. to 63 keV.⁷⁾ On the other hand, the resonance parameters of ^{142}Ce are poorly known, although measurements were made by Newson et al. in 1959,⁸⁾ and Vertebny et al. in 1970.⁹⁾ Cerium isotopes situate at a steep slope of the 4s peak of s-wave strength function. In addition, ^{140}Ce is a neutron magic nucleus($N=82$). For the applied purpose, cerium is included in the ^6Li -glass neutron scintillator as an activator(atomic ratio $\sim 10^{-3}$), so its cross section, especially at an 1.2 keV resonance region, is important for accurate efficiency calculations. Also cerium isotopes are fission product nuclei, their cross sections are related to reactor design.

We have made a series of transmission and capture measurements using a TOF facility of the JAERI linac, on many elements including separated isotope samples during period from 1982 to 1986. Resonance parameters and total cross sections deduced have been sent to NEA DATA BANK, and are compiled in a reference data book, "Neutron Cross Sections", Vol 1¹⁰⁾ and Vol 2¹¹⁾. A part of work on antimony was reported in a progress report,¹²⁾ and that on cerium was already published in the proceedings of the Int. Conf. on Nuclear Data, held at Santa Fe in 1985.¹³⁾

2. Measurements and Analyses

Transmission measurements were carried out at a 47-m TOF station of the JAERI electron linac,^{14,15)} a bird's eye view of which is shown in Fig.1. The linac produced pulsed electron beam of which energy was 120 MeV, peak current $\sim 3\text{A}$, pulse width 25ns and repetition rate 600 pps. Neutrons were produced at a water cooled tantalum target bombarded by the electron beam, and were moderated by a surrounding moderator. The target-moderator system

is described in the reference 16. The pulsed neutrons traversed to the TOF station through the evacuated flight tube. In the station, as shown in Fig.2, a ${}^6\text{Li}$ -glass transmission type neutron flux monitor was placed. At 1 m downstream from the monitor, a transmission sample was placed where the neutron beam was collimated to 35 mm in diameter. At 1.5 m downstream from the sample, a ${}^6\text{Li}$ -glass main detector(38mm ϕ x 12.7mm, NE912) was placed in a boron-paraffine shielding, an inner wall of which was lined with a B_4C layer of 1 cm thickness. A boron nitride filter was inserted in the beam to cut off slow neutrons which overlapped to the subsequent neutron bursts.

To find out small resonances, neutron capture measurements were made with a 500 l liquid scintillation tank, which was installed in a 55-m TOF station¹⁷⁾. Neutron detection signals from these scintillators were amplified, sorted and sent to a computer room through double shielded coaxial cables. The neutron detection events of the main detector were accumulated in a 4096 channel time analyzer with the minimum channel width 31.25ns. The neutron pulses from the flux monitor were gated to count in the energy region from 0.3 to 1.1 keV.

The accumulated data were transferred to the FACOM-U200 mini-computer, and were finally stored in a disk memory of the large computer FACOM-M380 at the JAERI computing center. The data processing and resonance analyses were made through a remote terminal at the linac laboratory. The conditions of the measurements are shown in Table 1.

Sizes and thicknesses of antimony and cerium samples are shown in Table 2. All the separated isotope samples were rent from the Oak Ridge National Laboratory Isotope Pool. The natural antimony samples were metallic plates or powder, and the separated isotope samples were metallic powder. These powder samples were packed in aluminum cases of 40 mm inner diameter and 10, 20 or 30 mm thicknesses. Natural cerium and ${}^{142}\text{Ce}$ samples were oxide powder, were heated to 200 °C for 3 hrs. to eliminate moisture, and were packed in the aluminum cases of the same dimension described above. For the capture measurements on cerium, the oxide

powder was packed into aluminum foils and were pressed to 69 mm diameter and 3 mm thickness using a die.

Neutron transmissions for these samples were deduced from the ratio of the sample-in spectra to the open-beam spectrum with the normalization of neutron fluence, after subtraction of backgrounds. The backgrounds in these spectra were estimated from the counts at the black resonances of cobalt(132eV), manganese (337eV), aluminum(35 and 88 keV), and some of the saturated resonances of antimony and cerium. To deduce the total cross section from the transmission data on oxides , the oxygen cross section,

$\sigma_0 = (3.85 - 0.002 E) \text{ barn} \quad (E < 200 \text{ keV})$
 was subtracted, where E is neutron energy in keV.¹⁸⁾ Energy scale of the TOF system was calibrated using the aluminum resonances at 5.9035 and 119.75 keV by adjusting the initial delay time of the analyzer system. The accuracy of the neutron flight path length was less than 1×10^{-4} . The neutron cross sections thus obtained include the Doppler broadening and resolution broadening due to the measuring system.

The resonance parameters (resonance energies and reduced neutron widths) of ^{121}Sb and ^{123}Sb were deduced by analysing the transmission data with a modified single level Atta-Harvey area analysis program. For ^{140}Ce and ^{142}Ce , the resonance parameters were deduced by a multi-level shape fit program SIOB¹⁹⁾, and in some cases a single level area analysis program.

3. Results of Analyses

3.1 Antimony

The raw data of the neutron time of flight spectra for the open beam (without any sample), and transmissions for the natural antimony are shown in Fig.3, where the energy region is from 125 to 720 eV and the sample thicknesses are 5, 10 and 35 mm. The raw

powder was packed into aluminum foils and were pressed to 69 mm diameter and 3 mm thickness using a die.

Neutron transmissions for these samples were deduced from the ratio of the sample-in spectra to the open-beam spectrum with the normalization of neutron fluence, after subtraction of backgrounds. The backgrounds in these spectra were estimated from the counts at the black resonances of cobalt(132eV), manganese (337eV), aluminum(35 and 88 keV), and some of the saturated resonances of antimony and cerium. To deduce the total cross section from the transmission data on oxides , the oxygen cross section,

$\sigma_0 = (3.85 - 0.002 E) \text{ barn} \quad (E < 200 \text{ keV})$
 was subtracted, where E is neutron energy in keV.¹⁸⁾ Energy scale of the TOF system was calibrated using the aluminum resonances at 5.9035 and 119.75 keV by adjusting the initial delay time of the analyzer system. The accuracy of the neutron flight path length was less than 1×10^{-4} . The neutron cross sections thus obtained include the Doppler broadening and resolution broadening due to the measuring system.

The resonance parameters (resonance energies and reduced neutron widths) of ^{121}Sb and ^{123}Sb were deduced by analysing the transmission data with a modified single level Atta-Harvey area analysis program. For ^{140}Ce and ^{142}Ce , the resonance parameters were deduced by a multi-level shape fit program SIOB¹⁹⁾, and in some cases a single level area analysis program.

3. Results of Analyses

3.1 Antimony

The raw data of the neutron time of flight spectra for the open beam (without any sample), and transmissions for the natural antimony are shown in Fig.3, where the energy region is from 125 to 720 eV and the sample thicknesses are 5, 10 and 35 mm. The raw

data of the transmission measurements on ^{121}Sb from 5 to 180 eV are shown in Fig.4a, and from 85 to 700 eV in Fig.4b where a level cluster is shown at about 450 eV. The observed total cross section of ^{123}Sb from 100 eV to 1 keV is shown in Fig.5. Resonance capture gamma-ray yields for ^{121}Sb are shown in Fig.6 in the energy region from 140 to 570 eV.

Assuming all the levels are s-wave levels, the reduced neutron widths were determined for 188 levels of ^{121}Sb , and for 202 levels of ^{123}Sb up to 5.3 keV, and are listed in Table 3 and 4, respectively. The reduced neutron widths of ^{121}Sb from 2.5 keV to 5.3 keV, and of ^{123}Sb from 4.1 keV to 5.3 keV are newly determined. The plot of cumulative number of levels vs. neutron energy for ^{121}Sb is shown in Fig.7, and for ^{123}Sb in Fig.8, changing cut-off values of $g \Gamma_n^0$ as described in the previous work.¹⁵⁾ From these figures, average level spacings for mixed ensembles of s- and p-wave levels were deduced to be

$$^{121}\text{Sb} \quad D = 10.3 \pm 0.5 \text{ eV} \quad E < 0.6 \text{ keV}$$

$$^{123}\text{Sb} \quad D = 20 \pm 1 \text{ eV} \quad E < 1.3 \text{ KeV}$$

where the missing levels may be small in these energy regions.

Cumulative values of $g \Gamma_n^0$ vs. neutron energy for ^{121}Sb are shown in Fig.9, and for ^{123}Sb in Fig.10. The s-wave strength functions S_0 were deduced to be

$$^{121}\text{Sb} \quad S_0 = (0.24 \pm 0.03) 10^{-4} \quad E < 5.3 \text{ keV},$$

$$^{123}\text{Sb} \quad S_0 = (0.25 \pm 0.03) 10^{-4} \quad E < 5.3 \text{ keV}.$$

which are nearly the same values. There seems a bump for ^{121}Sb in 1 to 3 keV region, and for ^{123}Sb up to 5 keV region an undulation with a period of about 1 keV. The previously compiled strength functions for these isotopes are somewhat different for the two isotopes; 0.3 ± 0.05 , and 0.25 ± 0.07 , respectively.¹⁰⁾ By the present measurement, it is proved that the difference is due to the local variation of the strength functions. A similar case is found in silver isotopes where the difference in previous values of the strength functions of ^{107}Ag and ^{109}Ag is much reduced by new measurements in a wider energy region.²⁰⁾

3.2 Cerium

The raw data of the neutron time spectra of the open beam, and the cerium sample-in are shown in Fig.11. The observed total cross sections of ^{140}Ce and those of ^{142}Ce were deduced from the transmission data of the $^{\text{nat}}\text{Ce}$ and ^{142}Ce samples which contained both nuclides in different ratios. The total cross sections of ^{140}Ce from 1 keV to 100 keV are shown in Figs.12a to 12d. A large resonance appears at 21.6 keV with a peak cross section 120 barn and a neutron width 600 eV. Similarly, the total cross sections of ^{142}Ce from 0.2 to 100 keV are shown in Figs.13a to 13f. The peak cross section of 1.27 KeV resonance of ^{142}Ce is observed to be 2000 barn, and the potential-resonance interference minimum is observed at 600 ± 100 eV, as shown in Fig.13a. In addition, very small levels, which are probably p-wave, are observed by the capture gamma ray detection with the 500 l liquid scintillation tank, six levels in ^{140}Ce and twelve levels in ^{142}Ce . The capture raw data for the ^{142}Ce and $^{\text{nat}}\text{Ce}$ samples are shown in Fig.14.

The reduced neutron widths of ^{140}Ce were deduced for the 15 levels up to 55 keV and are listed in Table 5. They are in good agreement with the previously reported values.^{1,7)} For ^{142}Ce the reduced neutron widths were deduced for the 38 levels below 50 keV, and are listed in Table 6. Most of them are newly determined. In Fig.15, a curve fitting to the transmission data by the SIOB is shown for resonances of ^{142}Ce from 20 to 37 keV.

The plots of the cumulative number of levels vs. neutron energy for ^{140}Ce is shown in Fig.16 and for ^{142}Ce in Fig.17, changing the cut-off value of Γ_n^0 . From these figures, the average level spacings for probable s-wave levels are deduced to be

$$^{140}\text{Ce} \quad D_0 = 3.5 \pm 0.8 \text{ keV} \quad E < 50 \text{ keV} \quad \Gamma_n^0 > 50 \text{ meV}$$

$$^{142}\text{Ce} \quad D_0 = 2.3 \pm 0.2 \text{ keV} \quad E < 50 \text{ keV} \quad \Gamma_n^0 > 50 \text{ meV}$$

If all small resonances (probable p-wave) are included, the average spacing of ^{142}Ce becomes 0.45 ± 0.1 keV.

The plots of the cumulative values of Γ_n^0 vs. neutron energy for ^{140}Ce are shown in Fig.18, and for ^{142}Ce in Fig.19. For ^{140}Ce , it is difficult to deduce definite value of s-wave strength function s_0 because of uncertain treatment of the large resonance at 21.6

keV.

If the 21.6 keV resonance is excluded, the s_0 value is

$$^{140}\text{Ce} \quad s_0 = (1.2 \pm 0.4) \times 10^{-4} \quad E < 50 \text{ keV}$$

If the 21.6 keV resonance is included, S_0 becomes to be

$$^{140}\text{Ce} \quad s_0 = (1.6 \pm 0.5) \times 10^{-4} \quad E < 50 \text{ keV}$$

It is interesting that s_0 below 20 keV is about the same value to that in the region above 22 KeV, as shown in Fig.18. Camarda¹⁾ reported that the s_0 value is nearly constant of 1.1×10^{-4} in the energy region from 22 keV to 250 keV, excluding the 21.6 KeV resonance.

For ^{142}Ce , the s-wave strength function is estimated from Fig.19 to be

$$^{142}\text{Ce} \quad s_0 = (2.7 \pm 0.6) \times 10^{-4} \quad E < 50 \text{ keV}$$

This value is about 2 times larger than that of ^{140}Ce . The s_0 values add new data points which depict the 4s peak of the strength function.

4.Discussions

The prominent property of the 21.6 keV resonance of ^{140}Ce in the compound nuclear state of ^{141}Ce may be due to N=82 closed shell effect, where the residual interaction is so weak that a simple structure is still remained even above the neutron threshold. For ^{142}Ce there seems leaps at 1.3, 24, and 43 keV, indicating strong levels at these energies. Similar anomalous leaps are found in the vicinity of the neutron closed shell nuclei, such as $^{81}\text{Br}^{21)}$, $^{87}\text{Rb}^{15})$, $^{139}\text{La}^{2})$, $^{141}\text{Pr}^{4})$, and many Pb isotopes.

From the effect of the leap in the strength functions of ^{140}Ce , it may be suggested that regular level series for the s-wave levels in ^{140}Ce can be found around the 21.6 keV, as shown in Fig.20. Although the decomposition is not unique, some series of spacings 3.5--6.6--5.5--6.6--3.5 (keV) or its fractions appear

keV.

If the 21.6 keV resonance is excluded, the s_0 value is

$$^{140}\text{Ce} \quad s_0 = (1.2 \pm 0.4) \times 10^{-4} \quad E < 50 \text{ keV}$$

If the 21.6 keV resonance is included, S_0 becomes to be

$$^{140}\text{Ce} \quad s_0 = (1.6 \pm 0.5) \times 10^{-4} \quad E < 50 \text{ keV}$$

It is interesting that s_0 below 20 keV is about the same value to that in the region above 22 KeV, as shown in Fig.18. Camarda¹⁾ reported that the s_0 value is nearly constant of 1.1×10^{-4} in the energy region from 22 keV to 250 keV, excluding the 21.6 KeV resonance.

For ^{142}Ce , the s-wave strength function is estimated from Fig.19 to be

$$^{142}\text{Ce} \quad s_0 = (2.7 \pm 0.6) \times 10^{-4} \quad E < 50 \text{ keV}$$

This value is about 2 times larger than that of ^{140}Ce . The s_0 values add new data points which depict the 4s peak of the strength function.

4.Discussions

The prominent property of the 21.6 keV resonance of ^{140}Ce in the compound nuclear state of ^{141}Ce may be due to N=82 closed shell effect, where the residual interaction is so weak that a simple structure is still remained even above the neutron threshold. For ^{142}Ce there seems leaps at 1.3, 24, and 43 keV, indicating strong levels at these energies. Similar anomalous leaps are found in the vicinity of the neutron closed shell nuclei, such as $^{81}\text{Br}^{21)}$, $^{87}\text{Rb}^{15})$, $^{139}\text{La}^2)$, $^{141}\text{Pr}^4)$, and many Pb isotopes.

From the effect of the leap in the strength functions of ^{140}Ce , it may be suggested that regular level series for the s-wave levels in ^{140}Ce can be found around the 21.6 keV, as shown in Fig.20. Although the decomposition is not unique, some series of spacings 3.5--6.6--5.5--6.6--3.5 (keV) or its fractions appear

overlappingly. Between these spacings, integer ratios appear: $3.5/5.5=7/11$, and $5.5/6.6=5/6$. The nearest neighbour level spacing distribution in the region shows a peak at 3.5 keV as shown in Fig.20. These series suggest some regular splitting pattern in the neutron resonance region. Moreover, the ratios of the resonance energies are integer ratios for the resonances around the 21.6 keV resonance: $21.6/9.53 = 9/4$, $21.6/18.06 = 6/5$, $21.6/24.76 = 7/8$, $21.6/28.19 = 10/13$, and so on.

In the resonance levels of ^{123}Sb , a Fourier like analysis of the level dispositions showed peaks at the integer multiples of 5.5 eV, previously reported by Ideno et al.³⁾ The present measurements have improved the accuracy of the resonance energies, and in fact, a long level series with energy at $E_n = 88(n + 1/2)$ (eV) ($n=1,2,\dots,8$) is confirmed, as shown in Fig.21. This series starts at 132 eV and stops at the 749 eV resonances.

In the real neutron resonances, integer multiples of 11 eV (or its simple integer ratios) appear frequently for many nuclei.^{3,22,23)} However, these structures do not show apparent deviation from the ordinary statistical distributions, even if regular structures exist. One of the author(M.O.) thinks that the regular patterns in resonance levels, and the integer ratios in resonance energies are general features of slow neutron resonances, though the physical meaning of these regular series is not yet clear. These regular series in neutron resonances may be related to the general features of chaotic system of highly excited compound nucleus. The analysis of the neutron resonances may reveal a new standpoint for new quantum physics.

Acknowledgments

The authors wish to thank the operator crew of the linac for the production of intense neutron beam. We also wish to thank the staffs of DOE and of Isotope Pool of Oak Ridge National Laboratory for the procuration of separated isotopes.

overlappingly. Between these spacings, integer ratios appear: $3.5/5.5=7/11$, and $5.5/6.6=5/6$. The nearest neighbour level spacing distribution in the region shows a peak at 3.5 keV as shown in Fig.20. These series suggest some regular splitting pattern in the neutron resonance region. Moreover, the ratios of the resonance energies are integer ratios for the resonances around the 21.6 keV resonance: $21.6/9.53 = 9/4$, $21.6/18.06 = 6/5$, $21.6/24.76 = 7/8$, $21.6/28.19 = 10/13$, and so on.

In the resonance levels of ^{123}Sb , a Fourier like analysis of the level dispositions showed peaks at the integer multiples of 5.5 eV, previously reported by Ideno et al.³⁾ The present measurements have improved the accuracy of the resonance energies, and in fact, a long level series with energy at $E_n = 88(n + 1/2)$ (eV) ($n=1,2,\dots,8$) is confirmed, as shown in Fig.21. This series starts at 132 eV and stops at the 749 eV resonances.

In the real neutron resonances, integer multiples of 11 eV (or its simple integer ratios) appear frequently for many nuclei.^{3,22,23)} However, these structures do not show apparent deviation from the ordinary statistical distributions, even if regular structures exist. One of the author(M.O.) thinks that the regular patterns in resonance levels, and the integer ratios in resonance energies are general features of slow neutron resonances, though the physical meaning of these regular series is not yet clear. These regular series in neutron resonances may be related to the general features of chaotic system of highly excited compound nucleus. The analysis of the neutron resonances may reveal a new standpoint for new quantum physics.

Acknowledgments

The authors wish to thank the operator crew of the linac for the production of intense neutron beam. We also wish to thank the staffs of DOE and of Isotope Pool of Oak Ridge National Laboratory for the procuration of separated isotopes.

References

- 1) H.S.Camarda:Phys.Rev.C18,1254(1978)
- 2) Hacken: Phys.Rev.C 13,1884(1976)
- 3) K.Ideno and M.Ohkubo: J.Phys.Soc.Japan: 30,620(1970)
- 4) S.Wynchank,J.B.Garg, W.W.Havens, and J.Rainwater: Phys.Rev.166,1234(1968)
- 5) G.V.Muradyan, Yu.V.Adamchuk and Yu.G.Shchepkin: Yader.Fiz.8,852(1968) transl. Sov.J.Nucl.Phys. 8,495(1969)
- 6) M.Ohkubo, Y.Nakajima, A.Asami, and T.Fuketa: J.Phys.Soc.Japan 33,1185(1975)
- 7) A.R.de L.Musgrove, B.J.Allen and R.L.Macklin : Aust.J.Phys.32,213(1979)
- 8) H.W.Newson, R.C.Block, P.F.Nichols, A.Taylor, A.K.Furr and E.Merzbacher: Ann.Phys.8,211(1959)
- 9) V.P.Veretebny, P.M.Vorona, O.I.Kalchenko, M.V.Paschunuk, F.I.Pusanko, V.A.Pshunuchuni and V.K.Rubushin : J.UFZ.15,2049(1970)
- 10) S.F.Mughabghab,M.Divadeenam and N.E.Holden ed.: "Neutron Cross Sections", Vol 1, Neutron Resonance Parameters and Thermal Cross Sections, Part A, Academic Press (1981)
- 11) V.Mclane, C.L.Dunford and P.F.Rose ed.: "Neutron Cross Sections" Vol 2, Neutron Cross Section Curves, Academic Press (1988)
- 12) M.Ohkubo: JAERI-M 87-115 (1987), p191
- 13) M.Ohkubo, M.Mizumoto, Y.Nakajima, M.Sugimoto, Y.Furuta and Y.Kawarasaki : Proc.Int.Conf. "Nuclear Data for Basic and Applied Science", Santa Fe, 1985, p1623 (Goldon-Breach 1986)
- 14) H.Takekoshi ed. JAERI-Report 1238(1975)
- 15) M.Ohkubo, M.Mizumoto and Y.Kawarasaki: J.Nucl.Sci.Technol. 21,254(1984)
- 16) M.Ohkubo: Nucl.Instr.Methods, A253, 43(1986)
- 17) M.Mizumoto, M.Sugimoto and T.Shoji: JAERI-M 84-211(1984)
- 18) M.Ohkubo: JAERI-M 86-193(1986)
- 19) G.de Saussure, D.K.Olsen and R.B.Perez: ORNL/TM-6286 (1978)
- 20) M.Mizumoto, M.Sugimoto, Y.Nakajima, M.Ohkubo,Y.Furuta and Y.Kawarasaki: J.Nucl.Sci.Technol. 20,883(1983)
- 21) M.Ohkubo, Y.Kawarasaki and M.Mizumoto: J.Nucl.Sci.Technol.

18,745(1981)

- 22) K. Ideno: J.Phys.Soc.Japan 37, 581(1974)
- 23) F.N.Belyaev and Borovlev: Sov.J.Nucl.Phys.27(2) 157,(1978)

Table 1 Condition of Measurements

Linac Electron Beam	120 MeV, ~3Å, 20 ns, 600 pps
Neutron Flight path	47-m station
Neutron Beam Diameter	35 mm ϕ
Neutron Detector	^6Li -glass (38mm ϕ x12.7mm t NE912)
Flux Monitor	^6Li -glass transmission type
Time Analyzer	4096 channels, 31.25ns
Computer	FACOM-M380

Table 2 Transmission Samples

samples	sizes (mm)	thickness (atoms/barn)	isotope composition
Sb nat	120 x 80 x 2	0.0038	121 57.25%
	150 x 150 x 5	0.0173	
	150 x 150 x10	0.0345	123 42.75
	150 x 150 x35	0.1165	
Sb-121	120 x 60 x 2	0.00266	121 99.57%
	40 ϕ x 10	0.0143	123 0.43
Sb-123	120 x 60 x 2	0.0020	121 0.95%
	40 ϕ x 10	0.0125	123 99.05
	20 ϕ x 50	0.0615	
Ce nat	69 ϕ x 3	0.0020	140 88.48%
	40 ϕ x 10	0.0060	
	40 ϕ x 30	0.0158	142 11.08
Ce-142	69 ϕ x 3	0.0022	140 7.89%
	40 ϕ x 20	0.0170	142 92.11

Table 3 Resonance Parameters of Sb-121

Energy (eV)	DE (eV)	$g\Gamma_{n^0}$ (meV)	$D(g\Gamma_{n^0})$ (meV)
10	6.22	0.01	0.04
	15.37	0.02	0.09
	29.58	0.02	0.05
	37.90	0.05	0.0003
	53.54	0.03	0.02
	55.00	0.05	0.0003
	64.45	0.04	0.005
	73.77	0.05	0.04
	89.58	0.07	0.06
	90.28	0.07	0.03
20	111.33	0.04	0.02
	126.60	0.05	0.10
	131.77	0.05	0.04
	144.13	0.06	0.06
	149.68	0.06	0.1
	160.40	0.07	0.01
	166.85	0.07	0.06
	184.45	0.10	0.003
	192.17	0.10	0.01
	213.81	0.11	0.01
30	222.42	0.11	0.02
	230.38	0.15	0.01
	245.80	0.15	0.005
	248.80	0.15	0.003
	261.50	0.16	0.008
	265.70	0.16	0.005
	269.90	0.16	0.003
	274.60	0.17	0.003
	286.09	0.18	0.05
	308.98	0.20	0.01
40	320.00	0.20	0.005
	330.78	0.21	0.01
	338.30	0.22	0.03
	343.80	0.25	0.01
	347.80	0.20	0.005
	355.70	0.20	0.003
	367.50	0.20	0.005
	392.57	0.28	0.10
	405.50	0.50	0.02
	414.40	0.20	0.005

Resonance Parameters of Sb-121

Energy (eV)	DE (eV)	$g\Gamma_{n^0}$ (meV)	$D(g\Gamma_{n^0})$ (meV)
50	420.92	0.31	0.05
	443.08	0.34	0.09
	447.25	0.34	0.08
	450.10	0.35	0.07
	453.55	0.35	0.40
	461.50	0.25	0.01
	469.60	0.19	0.03
	496.54	0.20	0.02
	499.90	0.20	0.007
	507.30	0.20	0.007
60	534.85	0.22	0.02
	542.62	0.23	0.21
	558.29	0.24	0.05
	563.31	0.50	0.01
	579.80	0.20	0.007
	598.62	0.26	0.01
	605.22	0.27	0.15
	613.04	0.28	0.02
	630.15	0.29	0.08
	660.57	0.31	0.06
70	670.35	0.31	0.07
	675.38	0.32	0.03
	709.87	0.35	0.04
	714.40	0.50	0.02
	718.22	0.36	0.07
	734.80	0.50	0.02
	771.60	0.39	0.10
	789.20	0.41	0.04
	794.41	0.41	0.08
	799.41	0.41	0.12
80	802.90	0.41	0.12
	837.75	0.45	0.05
	858.47	0.46	0.02
	889.10	0.48	0.02
	910.75	0.50	0.03
	916.17	0.51	0.20
	935.07	0.52	0.01
	946.60	0.53	0.08
	961.39	0.54	0.07
	992.77	0.57	0.20

Resonance Parameters of Sb-121

Energy (eV)	DE (eV)	$g\Gamma_n^0$ (meV)	$D(g\Gamma_n^0)$ (meV)
90	1011.7	0.58	0.04
	1035.3	0.61	0.01
	1045.9	0.62	0.01
	1083.8	0.65	0.05
	1109.9	0.67	0.18
	1144.3	0.71	0.02
	1179.6	1.00	0.15
	1182.7	1.00	0.15
	1200.8	0.76	0.10
	1219.3	0.78	0.05
100	1249.5	0.80	0.10
	1306.5	0.85	0.15
	1327.8	0.88	0.04
	1345.5	0.88	0.03
	1363.9	0.89	0.18
	1435.8	0.96	0.11
	1483.3	1.05	0.13
	1520.5	1.50	0.07
	1528.6	1.50	0.07
	1552.9	1.10	0.04
110	1572.0	1.10	0.02
	1593.4	1.20	0.16
	1638.4	1.20	0.05
	1697.3	1.30	0.10
	1721.5	1.30	0.03
	1773.8	1.40	0.09
	1788.2	1.40	0.02
	1796.6	1.40	0.10
	1818.5	1.50	0.10
	1822.5	1.50	0.10
120	1843.3	1.6	0.02
	1891.1	1.7	0.08
	1901.6	1.8	0.30
	1915.5	1.9	0.12
	1976.4	1.9	0.20
	1998.5	1.9	0.30
	2032.0	1.9	0.09
	2081.4	2.0	0.05
	2105.6	2.0	0.15
	2114.7	2.0	0.09

Resonance Parameters of Sb-121

Energy (eV)	DE (eV)	$g\Gamma_n^0$ (meV)	D($g\Gamma_n^0$) (meV)
2145.2	2.0	1.05	0.15
2186.0	2.1	0.15	0.05
2200.7	2.1	0.32	0.05
2219.6	2.2	0.50	0.08
2253.2	2.2	0.94	0.15
2266.1	2.2	0.36	0.06
2303.	2.2	1.12	0.16
2364.	2.2	1.38	0.20
2390.	2.4	1.49	0.22
130 2433.2	2.4	0.84	0.12
2460.	2.6	0.36	0.05
2524.7	2.6	4.16	0.60
2557.	2.6	0.82	0.10
2572.	2.7	0.20	0.05
2581.	2.7	0.30	0.08
2600.	2.7	0.45	0.10
2620.	2.8	0.34	0.10
2684.	2.8	0.97	0.20
2714.	2.8	0.30	0.10
140 2765.	2.9	0.76	0.20
2802.	3.0	0.16	0.10
2828.	3.0	0.38	0.10
2848.	3.0	1.10	0.20
2872.	3.1	0.60	0.15
2881.	3.1	0.50	0.15
2913.	3.1	2.40	0.20
2972.	3.2	0.48	0.15
2994.	3.3	2.52	0.30
3023.	3.3	0.30	0.10
150 3123.	3.4	0.20	0.10
3172.	3.6	0.33	0.10
3222.	3.6	0.20	0.10
3242.	3.6	0.36	0.10
3262.	3.7	1.35	0.30
3345.	3.8	1.49	0.30
3365.	3.8	0.38	0.10
3386.	3.9	0.38	0.10
3468.	4.0	0.86	0.20
3514.	4.1	1.26	0.30
160 3552.	4.1	2.00	0.50

Resonance Parameters of Sb-121

Energy (eV)	DE (eV)	$g\Gamma_n^0$ (meV)	D($g\Gamma_n^0$) (meV)
170	3562.	4.2	1.00
	3653.	4.5	1.00
	3706.	4.5	1.40
	3785.	4.5	0.40
	3837.	4.6	1.75
	3859.	4.7	0.68
	3911.	4.8	0.45
	3933.	4.8	0.67
	3968.	4.9	1.00
	3977.	4.9	2.00
180	4007.	5.0	0.67
	4115.	5.1	2.48
	4144.	5.2	0.86
	4208.	5.3	0.66
	4233.	5.4	0.78
	4279.	5.4	3.12
	4357.	5.5	1.13
	4458.	5.7	0.80
	4497.	5.8	0.70
	4508.	5.9	2.50
	4563.	6.0	0.70
	4745.	6.3	1.00
	4760.	6.4	2.50
	4862.	6.5	0.86
	5079.	6.9	4.15
	5227.	7.2	1.27
	5277.	7.3	2.33
	5350.	7.5	2.63
			0.50

Table 4 Resonance Parameters of Sb-123

Energy (eV)	DE (eV)	$g\Gamma_n^0$ (meV)	D($g\Gamma_n^0$) (meV)
10	21.37	0.02	3.25
	50.50	0.04	0.21
	76.70	0.05	0.33
	104.88	0.07	2.20
	130.85	0.08	0.046
	176.20	0.11	0.014
	185.90	0.11	0.013
	191.60	0.12	0.68
	197.50	0.12	0.018
	218.45	0.13	0.15
20	225.00	0.13	0.013
	240.35	0.14	0.64
	295.43	0.18	0.05
	298.90	0.18	0.66
	302.40	0.18	0.012
	323.20	0.19	1.05
	343.80	0.21	0.016
	350.85	0.21	0.18
	373.20	0.23	0.043
	394.26	0.24	0.66
30	413.70	0.25	0.022
	471.07	0.29	0.105
	481.31	0.30	0.32
	490.60	0.31	0.016
	519.50	0.33	0.025
	532.40	0.34	0.26
	550.50	0.35	0.012
	570.50	0.37	0.62
	592.00	0.38	0.018
	598.50	0.39	0.20
40	627.50	0.41	0.56
	644.30	0.42	0.04
	658.70	0.43	0.38
	690.90	0.46	0.10
	717.90	0.48	0.15
	746.50	0.51	2.80
	753.80	0.51	0.015
	785.40	0.54	0.016
	794.50	0.55	0.032
	815.00	0.56	0.55

Resonance Parameters of Sb-123

Energy (eV)	DE (eV)	$g\Gamma_n^o$ (meV)	D($g\Gamma_n^o$) (meV)
50	839.00	0.5	1.80
	853.50	0.6	0.015
	871.40	0.6	3.20
	884.40	0.6	1.40
	909.2	0.6	0.41
	929.0	0.7	0.25
	967.8	0.7	0.42
	976.7	0.7	0.10
	987.7	0.7	1.22
	1025.2	0.8	0.32
60	1034.9	0.8	0.027
	1047.9	0.8	0.75
	1064.4	0.8	0.027
	1083.3	0.8	0.21
	1109.3	0.8	0.27
	1116.6	0.8	0.70
	1120.70	0.9	0.025
	1124.8	0.9	0.034
	1164.7	0.9	1.30
	1220.7	1.0	0.03
70	1234.0	1.0	0.025
	1248.4	1.0	0.50
	1261.0	1.0	0.04
	1272.2	1.0	0.96
	1293.5	1.0	0.031
	1308.4	1.0	0.48
	1328.8	1.1	0.23
	1335.0	1.2	0.05
	1358.0	1.2	0.05
	1384.5	1.1	0.32
80	1419.5	1.2	0.068
	1456.3	1.2	0.11
	1482.0	1.2	2.75
	1489.8	1.2	1.20
	1493.0	1.2	0.55
	1567.0	1.3	0.10
	1598.8	1.4	0.46
	1618.2	1.4	1.60
	1646.5	1.4	0.52
	1670.2	1.4	0.17

Resonance Parameters of Sb-123

Energy (eV)	DE (eV)	$g\Gamma_n^0$ (meV)	$D(g\Gamma_n^0)$ (meV)
1697.0	1.5	2.40	0.25
1709.2	1.5	0.05	0.01
1731.3	1.5	0.10	0.01
1740.0	1.5	0.10	0.01
1781.0	1.6	0.90	0.09
1794.7	1.6	4.10	0.40
1826.5	1.6	0.25	0.03
1858.9	1.7	2.15	0.20
1869.2	1.7	1.75	0.18
90 1930.3	1.8	0.65	0.07
1964.0	1.8	0.13	0.01
1999.5	1.9	4.0	0.4
2034.2	1.9	0.16	0.02
2083.6	2.0	0.1	0.01
2105.4	2.0	0.7	0.07
2113.4	2.0	0.2	0.02
2144.7	2.0	0.6	0.06
2151.1	2.1	1.4	0.15
2163.4	2.1	0.3	0.03
100 2169.5	2.1	0.8	0.1
2191.8	2.1	0.15	0.02
2195.5	2.1	0.15	0.02
2202.3	2.1	0.37	0.04
2234.5	2.2	2.1	0.2
2258.8	2.2	0.1	0.01
2271.5	2.2	0.27	0.03
2304.5	2.3	0.35	0.04
2312.6	2.3	0.44	0.04
2353.6	2.3	1.10	0.1
110 2365.5	2.3	0.37	0.04
2384.3	2.4	0.34	0.04
2441.5	2.4	0.30	0.03
2469.0	2.5	0.30	0.03
2478.3	2.5	1.10	0.1
2536.7	2.6	0.3	0.03
2549.5	2.6	0.2	0.02
2566.3	2.6	0.3	0.03
2586.4	2.7	0.2	0.02
2627.7	2.7	0.15	0.02
120 2650.0	2.7	0.38	0.04

Resonance Parameters of Sb-123

Energy (eV)	DE (eV)	$g\Gamma_n^0$ (meV)	D($g\Gamma_n^0$) (meV)
2689.0	2.8	0.30	0.03
2702.1	2.8	1.40	0.14
2715.5	2.8	0.30	0.03
2739.2	2.9	0.20	0.02
2769.0	2.9	0.2	0.02
2773.5	2.9	0.2	0.02
2783.0	2.9	0.2	0.02
2823.0	3.0	0.91	0.09
2834.5	3.0	0.51	0.05
130 2866.0	3.1	0.20	0.02
2892.	3.1	1.50	0.15
2917.5	3.1	0.45	0.05
2940.5	3.2	0.30	0.03
2957.5	3.2	0.20	0.02
2970.0	3.2	0.35	0.04
2999.5	3.3	0.43	0.04
3016.2	3.3	1.90	0.20
3051.0	3.3	0.30	0.03
3064.	3.4	0.2	0.02
140 3077.	3.4	0.6	0.06
3118.	3.4	1.55	0.16
3144.	3.5	0.2	0.02
3158.	3.5	0.2	0.02
3198.	3.6	1.1	0.10
3232.	3.6	1.1	0.10
3253.	3.7	2.7	0.3
3304.	3.7	2.3	0.2
3348.	3.8	0.2	0.02
3366.	3.8	0.65	0.07
150 3395.	3.9	1.40	0.14
3405.	3.9	0.2	0.02
3442.	4.0	0.5	0.05
3517.	4.1	0.9	0.09
3534.	4.1	0.2	0.02
3575.	4.2	0.2	0.02
3610.	4.3	0.15	0.02
3638.	4.3	0.40	0.04
3656.	4.5	0.15	0.02
3680.	4.5	1.10	0.11
160 3692.	4.5	0.5	0.05

Resonance Parameters of Sb-123

Energy (eV)	DE (eV)	$g\Gamma_n^0$ (meV)	$D(g\Gamma_n^0)$ (meV)
3748.	4.5	0.30	0.03
3778.	4.5	0.30	0.03
3805.	4.6	0.55	0.06
3840.	4.6	0.30	0.03
3880.	4.7	0.85	0.09
3929.	4.8	0.30	0.03
3947.	4.8	0.3	0.03
3977.	4.9	3.0	0.3
4018.	5.0	0.2	0.02
170 4034.	5.0	0.35	0.04
4055.	5.0	0.15	0.02
4070.	5.0	0.15	0.02
4104.	5.1	1.25	0.12
4146.	5.2	4.2	0.42
4160.6	5.2	2.6	0.26
4217.	5.3	0.6	0.06
4276.	5.4	0.3	0.03
4306.	5.5	0.25	0.03
4345.	5.5	0.40	0.04
180 4376.	5.6	0.60	0.06
4401.	5.7	0.30	0.03
4424.	5.7	0.3	0.03
4454.	5.7	1.10	0.1
4485.	5.8	0.40	0.04
4573.	6.0	0.2	0.02
4616.	6.1	0.80	0.08
4650.	6.1	0.3	0.03
4679.	6.2	0.3	0.03
4691.	6.2	1.90	0.20
190 4711.	6.2	0.2	0.02
4777.	6.4	2.1	0.21
4869.	6.5	0.9	0.09
4944.	6.7	1.10	0.11
4980.	6.8	0.70	0.07
5005.	6.8	0.3	0.03
5033.	6.9	1.50	0.15
5060.	6.9	1.0	0.10
5141.	7.1	0.60	0.06
5215.	7.2	1.30	0.13
200 5270.	7.3	0.90	0.09
5320.	7.4	0.50	0.05
5347.	7.5	0.60	0.06

Table 5 Resonance Parameters of Ce-140

Energy (eV)	DE (eV)	Γ_n^0 (meV)	D(Γ_n^0) (meV)
2543.7	2.6	11.7	2.
6005.	9.	12.9	2.
+ 8400.	15.		
9568.	19.	530.	50.
11419.	24.	156.	20.
12473.	28.	322.	40.
+ 14000.	33.		
+ 16146.	41.		
+ 16420.	42.		
10 18167.	49.	660.	70.
21623.	64.	4100.	300.
+ 23200.	71.		
24798.	78.	360.	40.
28198.	95.	580.	60.
+ 29200.	100.		
30695.	107.	140.	20.
+ 34770.	129.		
38233.	149.	280.	40.
+ 39150.	155.		
20+ 40180.	161.		
41893.	171.	1250.	100.
+ 44800.	190.		
49484.	220.	400.	50.
53030.	244.	300.	40.
55113.	258.	840.	100.

+) very small probable p-wave levels.

Table 6 Resonance Parameters of Ce-142

	Energy (eV)	DE (eV)	Γ_n^0 (meV)	D(Γ_n^0) (meV)
+ 1152.	7 a)	0.8		
1277.	0.9	2000.	50.	
+ 1742.0	1.5	3.1	0.3	
+ 2793.	2.9	325.	25.	
+ 2941.	3.2			
+ 2966.	3.2			
+ 3835.	4.7	600.	32.	
+ 4295.	5.6	2.5	0.3	
+ 4525.	6.1	8.	1.	
10+ 5190.	7.5			
+ 5623.	8.4	15.	1.5	
+ 5816.	8.9	1.6	0.2	
+ 5966.	9.2			
+ 6429.	10.	2.9	0.3	
+ 7478.	13.			
+ 8149.	15.	40.	4.	
+ 8350.	15.			
+ 8401.	15.	210.	12.	
+ 8858.	17.			
20 9433.	18.	13.	1.5	
+ 9647.	19.			
+ 10891.	23.			
+ 10915.	23.	16.	2.	
+ 11177.	24.	100.	10.	
+ 11318.	24.	26.	3.	
+ 11970.	26.	30.	3.	
+ 12255.	27.			
+ 12486.	28.			
+ 12775.	29.	280.	20.	
30 13976.	33.	14.	2.	
+ 15225.	37.	760.	80.	
+ 16638.	43.	40.	5.	
+ 17298.	45.	95.	10.	
+ 17822.	48.	27.	3.	
+ 19414.	54.	10.	2.	
+ 20576.	59.	148.	15.	
+ 21173.	62.	15.	3.	
+ 22600.	68.	1080.	30.	
+ 23190.	71.	1270.	32.	
40 24740.	78.	360.	20.	

Resonance Parameters of Ce-142 (Contn.)

Energy (eV)	DE (eV)	Γ_n^0 (meV)	D(Γ_n^0) (meV)
25360.	81.	2150.	60.
29300.	100.	210.	25.
30880.	108.	170.	30.
38160.	149.	700.	60.
38890.	153.	190.	50.
39640.	158.	310.	30.
42725.	176.	300.	30.
43365.	180.	1770.	150.
49245.	218.	300.	50.

† very small probable p-wave levels.

a) 2.8 eV higher than the 1150 eV resonance of ^{56}Fe .

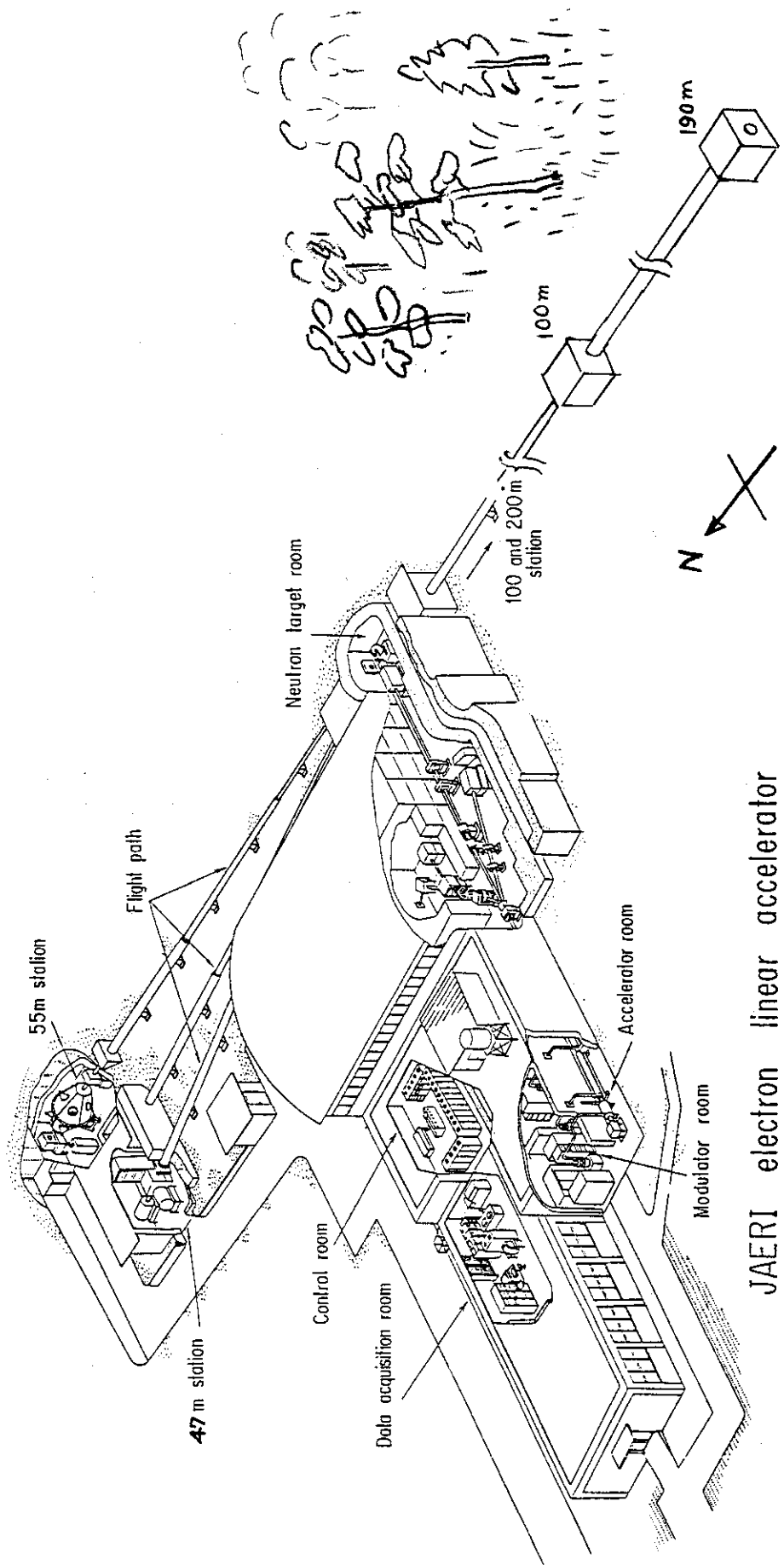
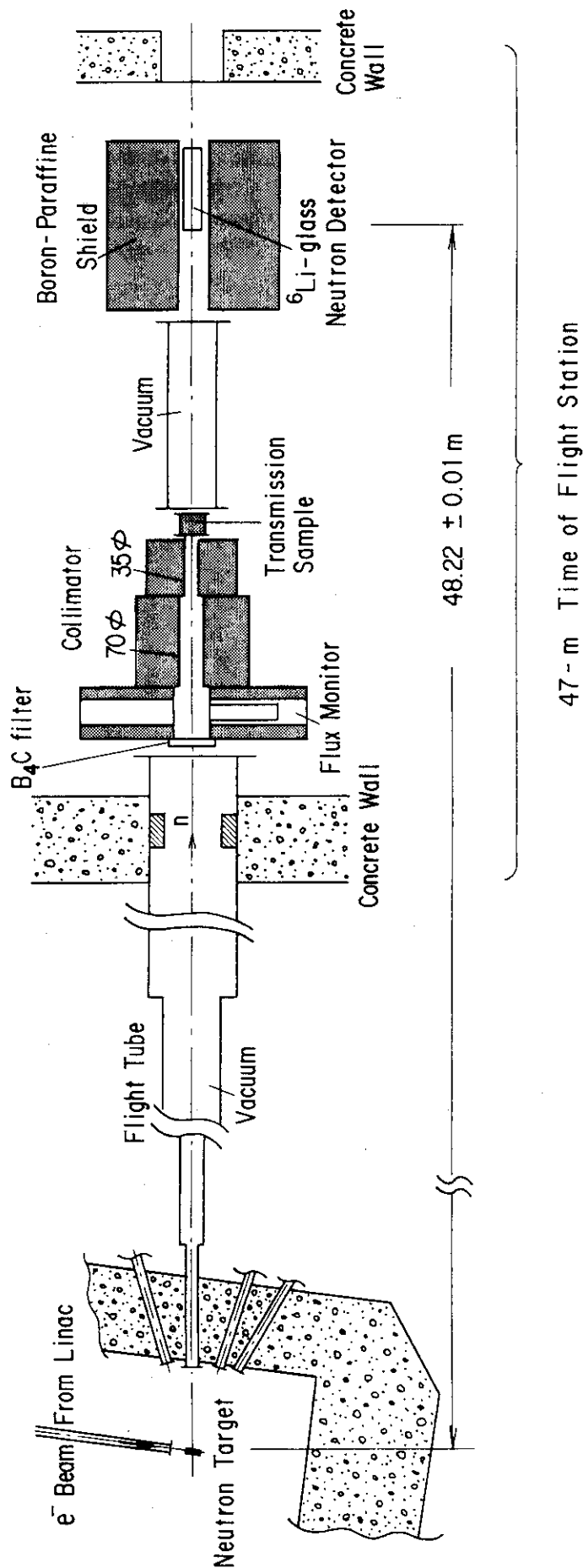


Fig. 1 A birds eye view of the JAERI Linac TOF spectrometer



47-m Time of Flight Station

Fig.2 Schematic figure of the 47-m TOF station. Pulsed neutrons came from left side. The neutrons were detected by a ^{6}Li glass detector in a shielding. Upstream the detector, a BN filter and a neutron flux monitor and transmission samples were placed in a $35\text{mm}\phi$ collimated neutron beam.

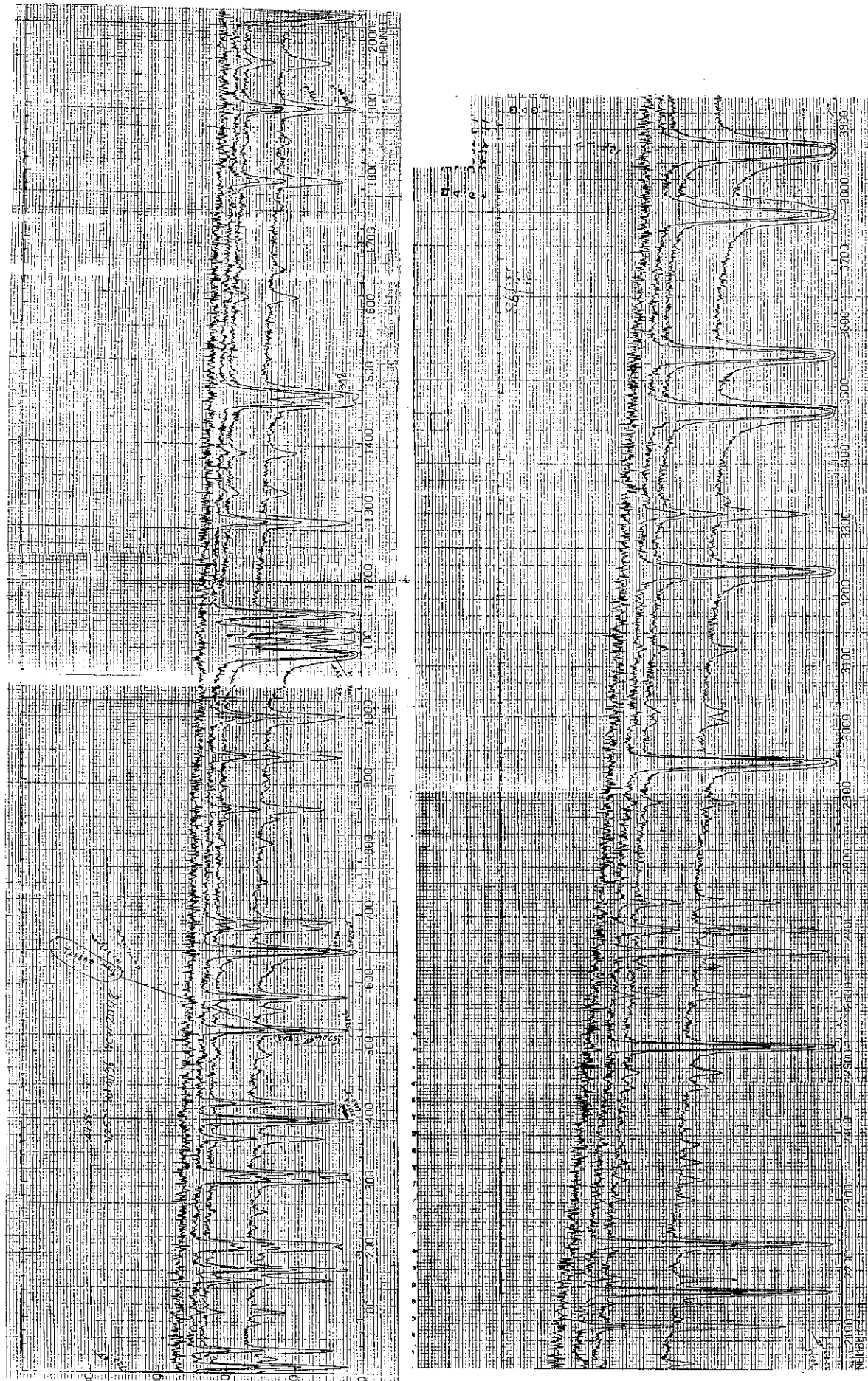


Fig. 3 Raw data of neutron time spectra for open beam (without sample), and for natural antimony of 5, 10, and 35 mm thicknesses in the beam, in energy region from 125 to 720 eV. The time channel width are 31.25 ns for 1st half, and 62.5ns for 2nd half of the 4096 analyzer.

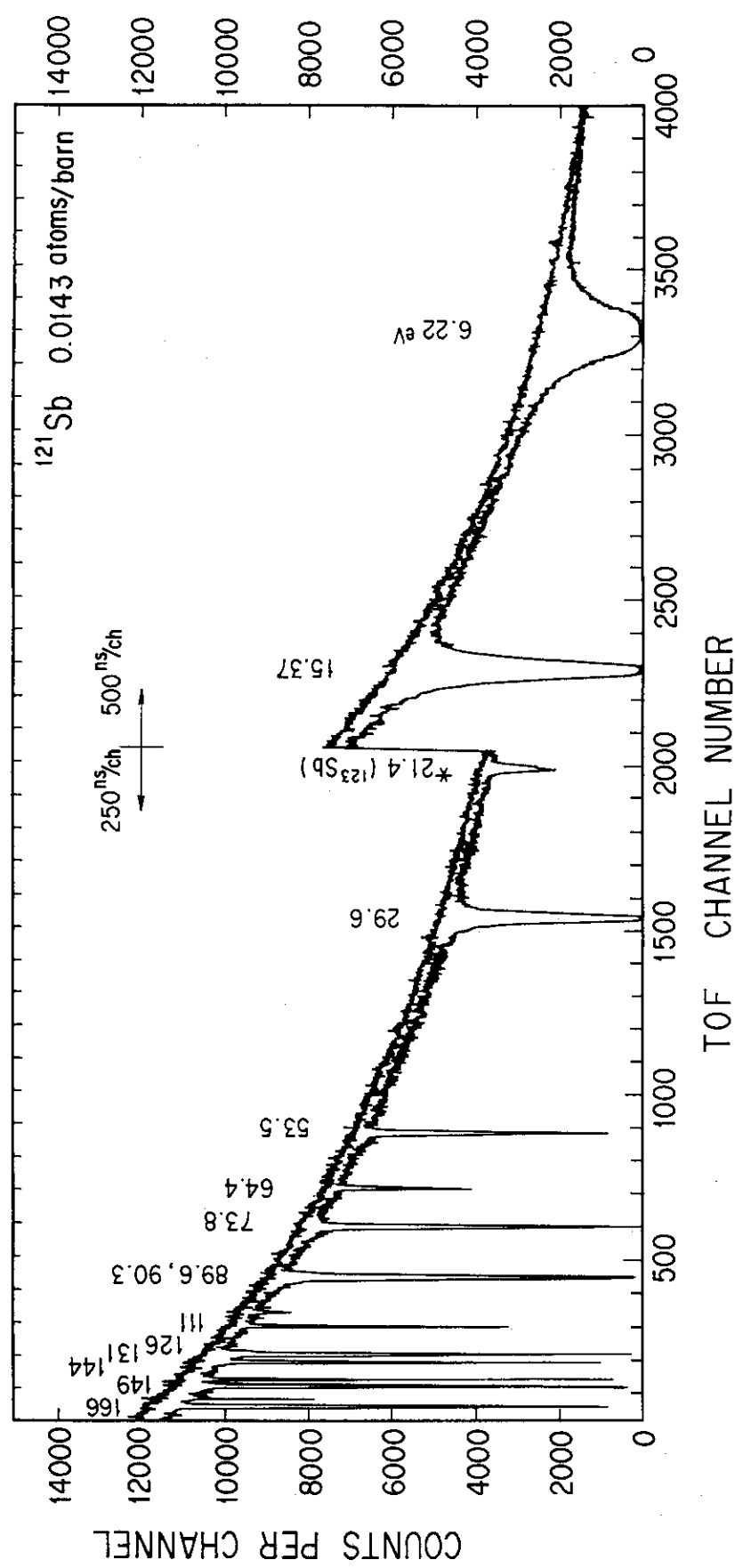


Fig. 4a Raw data of transmission measurements on ^{121}Sb from 5 eV to 170 eV, with sample thickness 0.0143 atoms/barn. The time channel widths are 250 ns for left half and 500 ns for right half, respectively. Open beam is also shown.

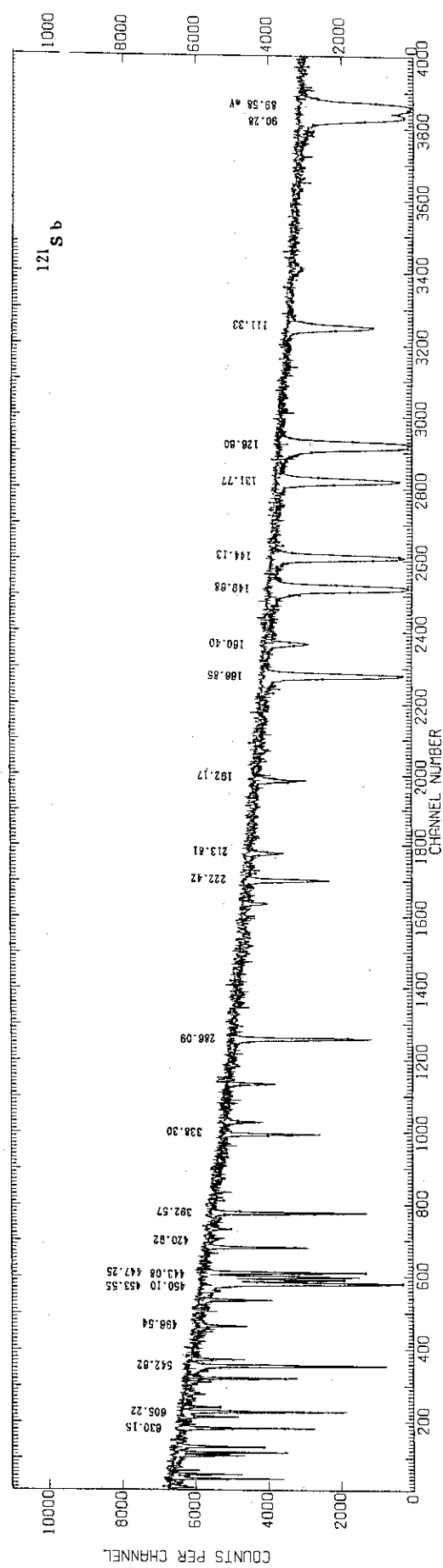
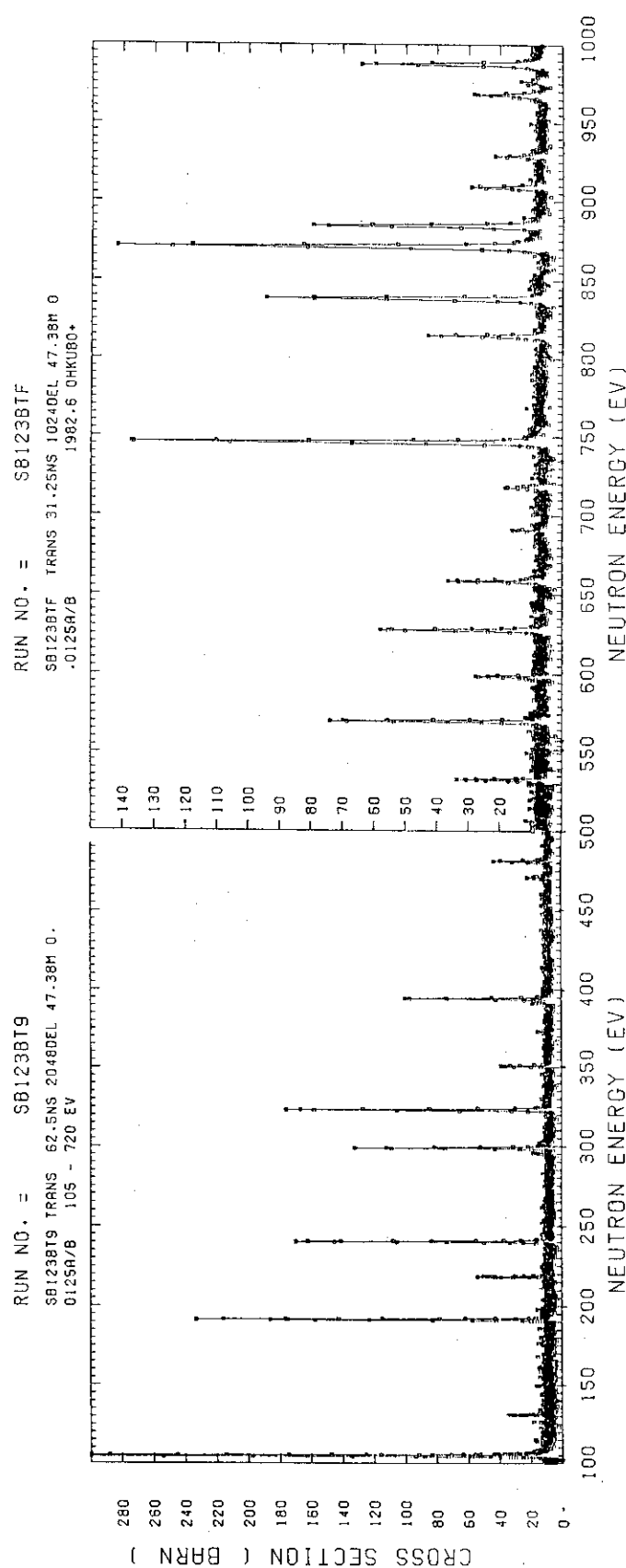


Fig.4b Raw data of transmission measurements on ^{121}Sb from 85 eV to 700 eV with sample thickness 0.0143 atoms/barn. The time channel is 62.5 ns. At about 450 eV, a cluster composed of four strong resonances is seen. Open beam is also shown.

Fig. 5 Total cross section of ^{123}Sb from 100 to 1000 eV deduced from the transmission data.

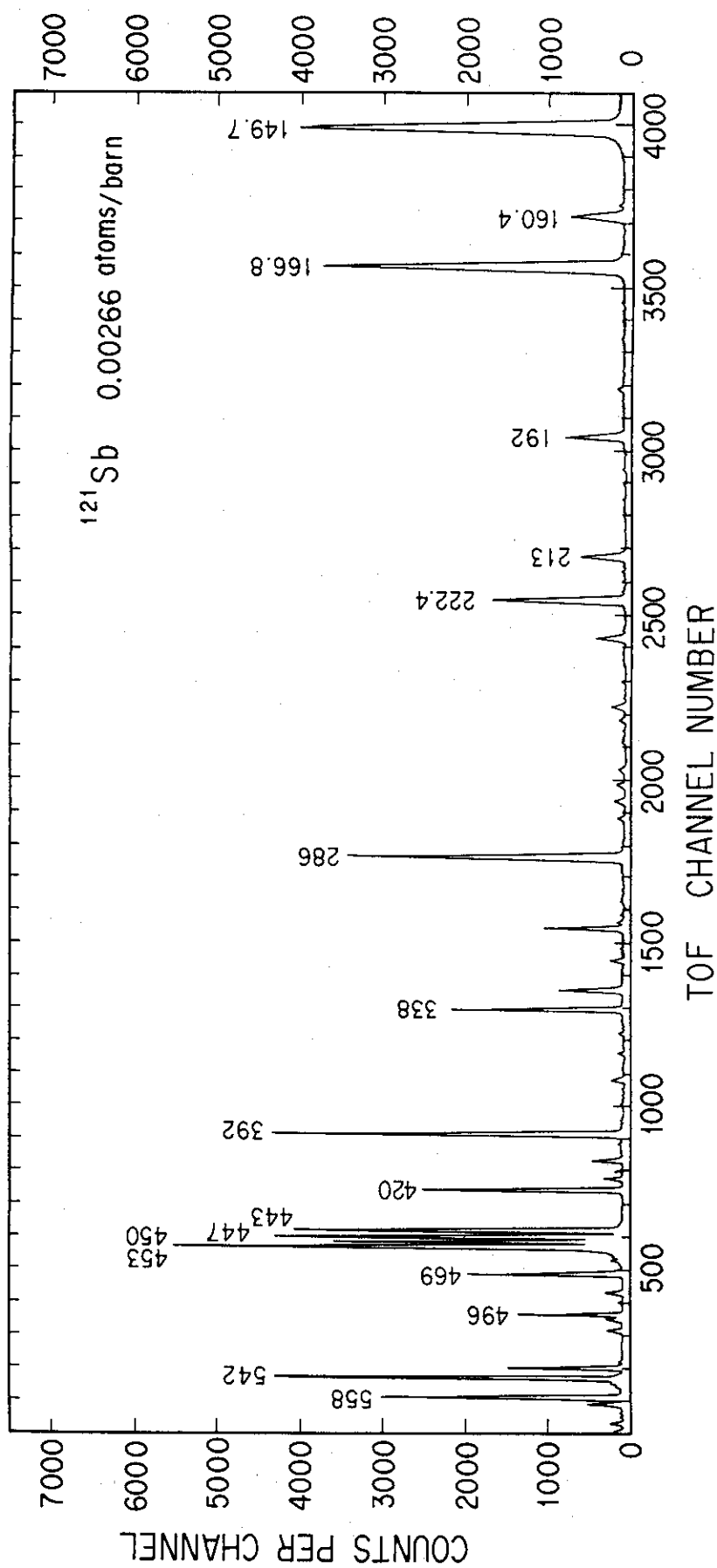


Fig. 6 Resonance capture yields for ^{121}Sb in the energy region from 145 eV to 580 eV measured by the 500 l liquid scintillator tank. A cluster of resonances at about 450 eV are seen.

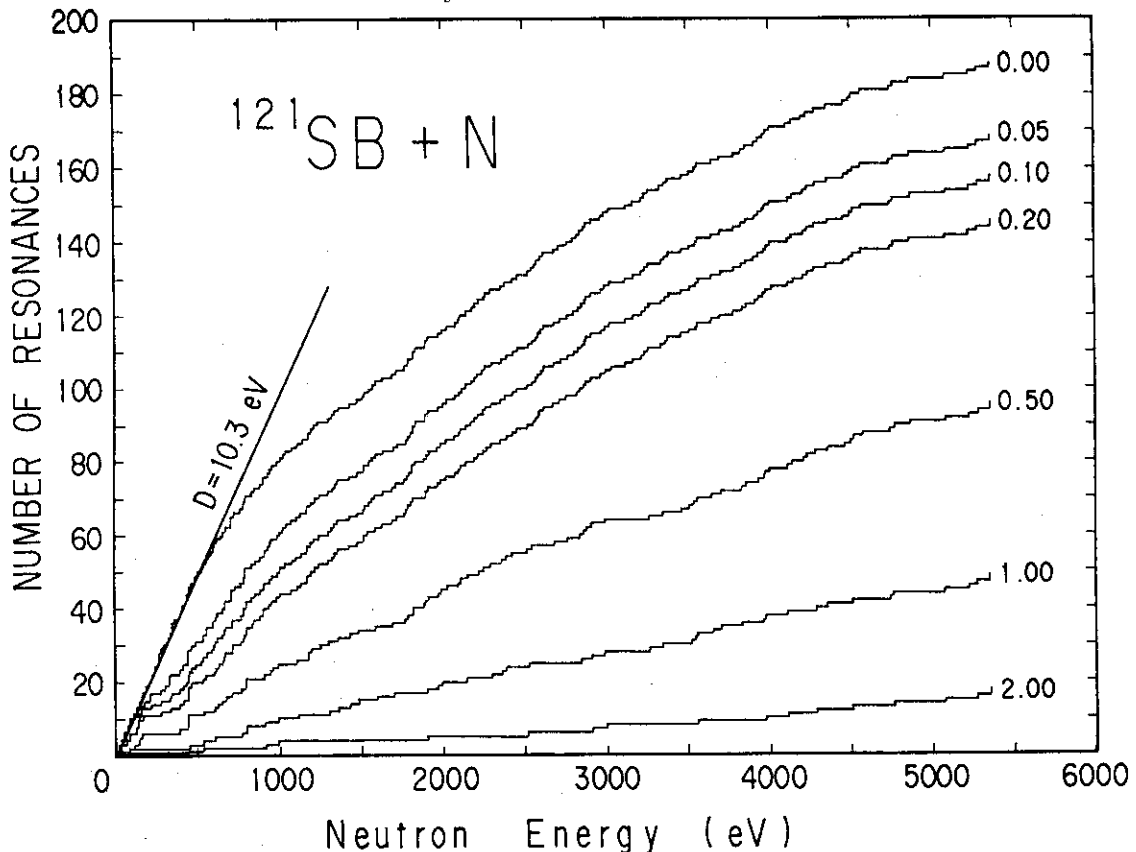


Fig. 7 Cumulative number of ^{121}Sb resonances versus neutron energy, with several cut off threshold in $g\Gamma_n^0$ values. Average spacing for s wave levels is deduced to be $D = 10.3 \pm 0.5 \text{ eV}$.

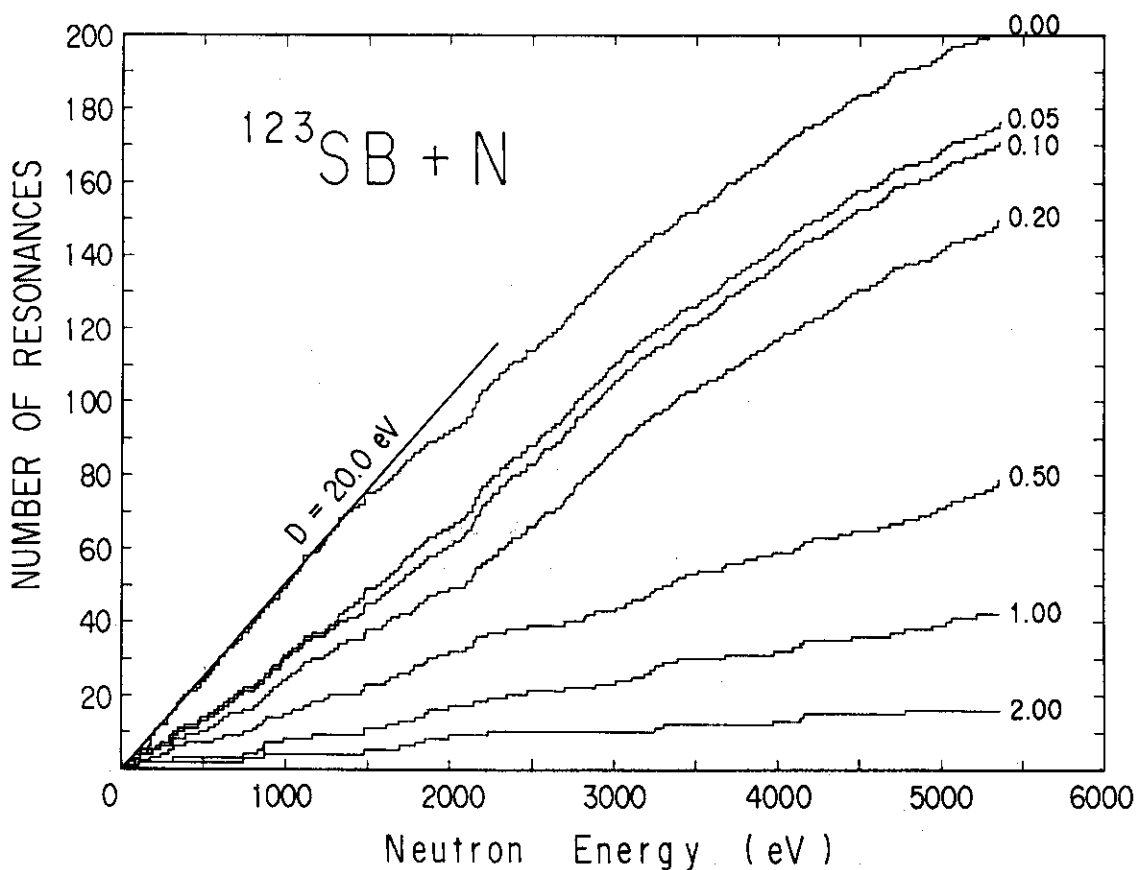


Fig. 8 Cumulative number of ^{123}Sb resonances versus neutron energy, with several cut off threshold in $g\Gamma_n^0$ values. Average spacing for s wave levels is deduced to be $D = 20 \pm 1 \text{ eV}$.

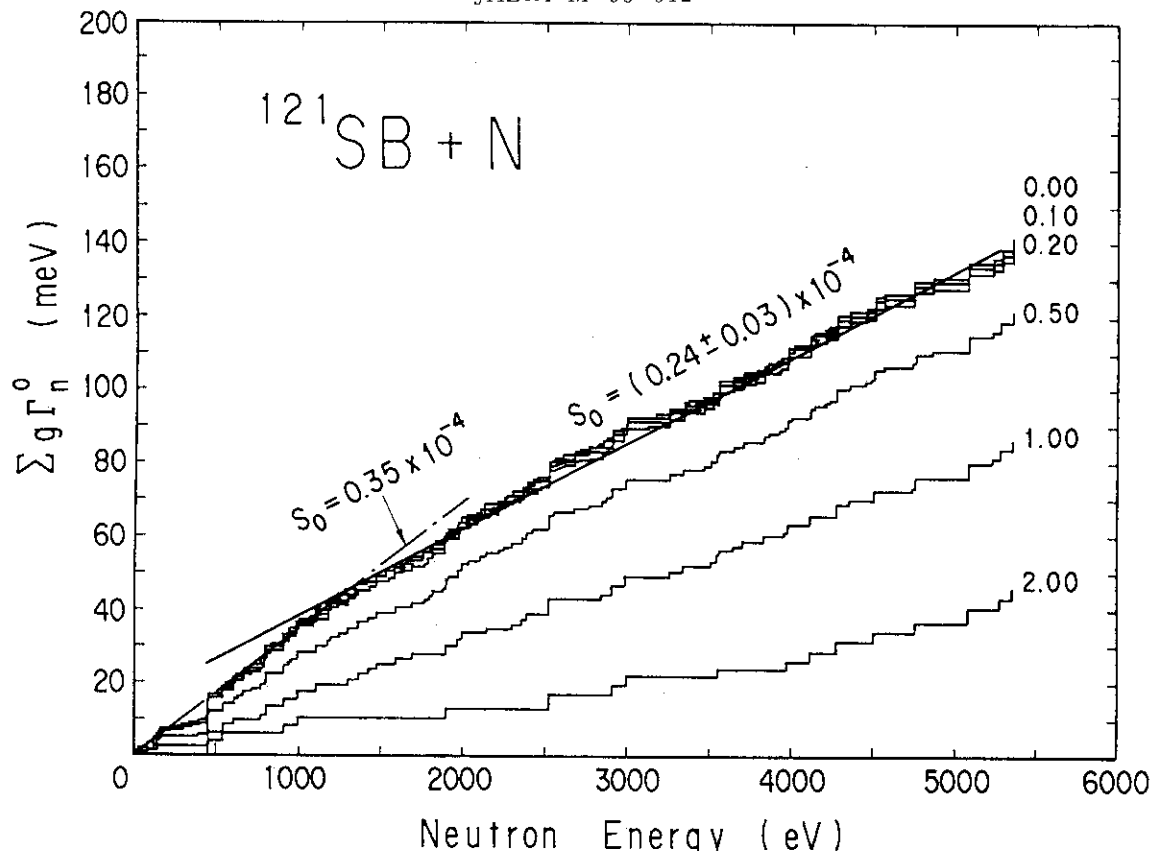


Fig. 9 Cumulative values of $g\Gamma_n^0$ versus neutron energy for ^{121}Sb . In the region from 1 keV to 5 keV, S_0 is deduced to be $(0.24 \pm 0.03)^{-4}$, whereas below 1 keV, it is somewhat large value of 0.35×10^{-4} .

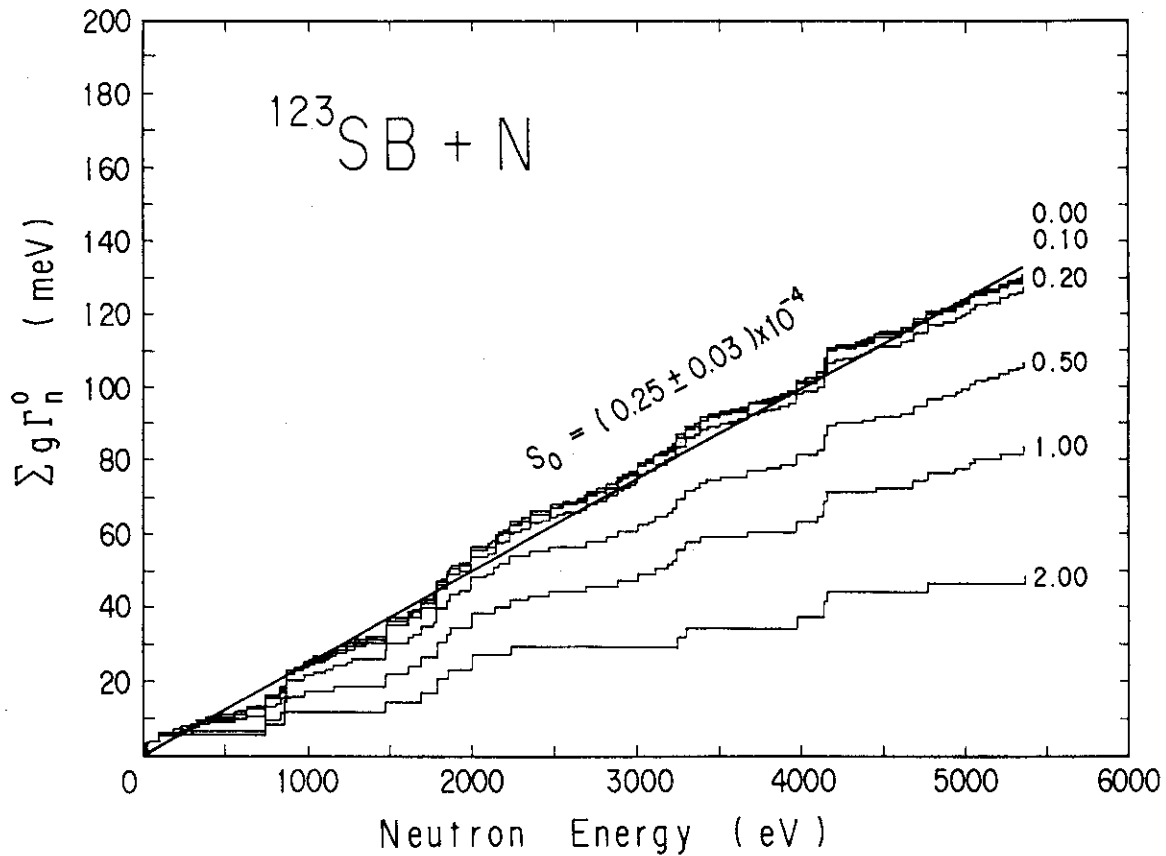


Fig. 10 Cumulative values of $g\Gamma_n^0$ versus neutron energy for ^{123}Sb . S_0 is deduced to be $(0.25 \pm 0.03) \times 10^{-4}$ below 5 keV.

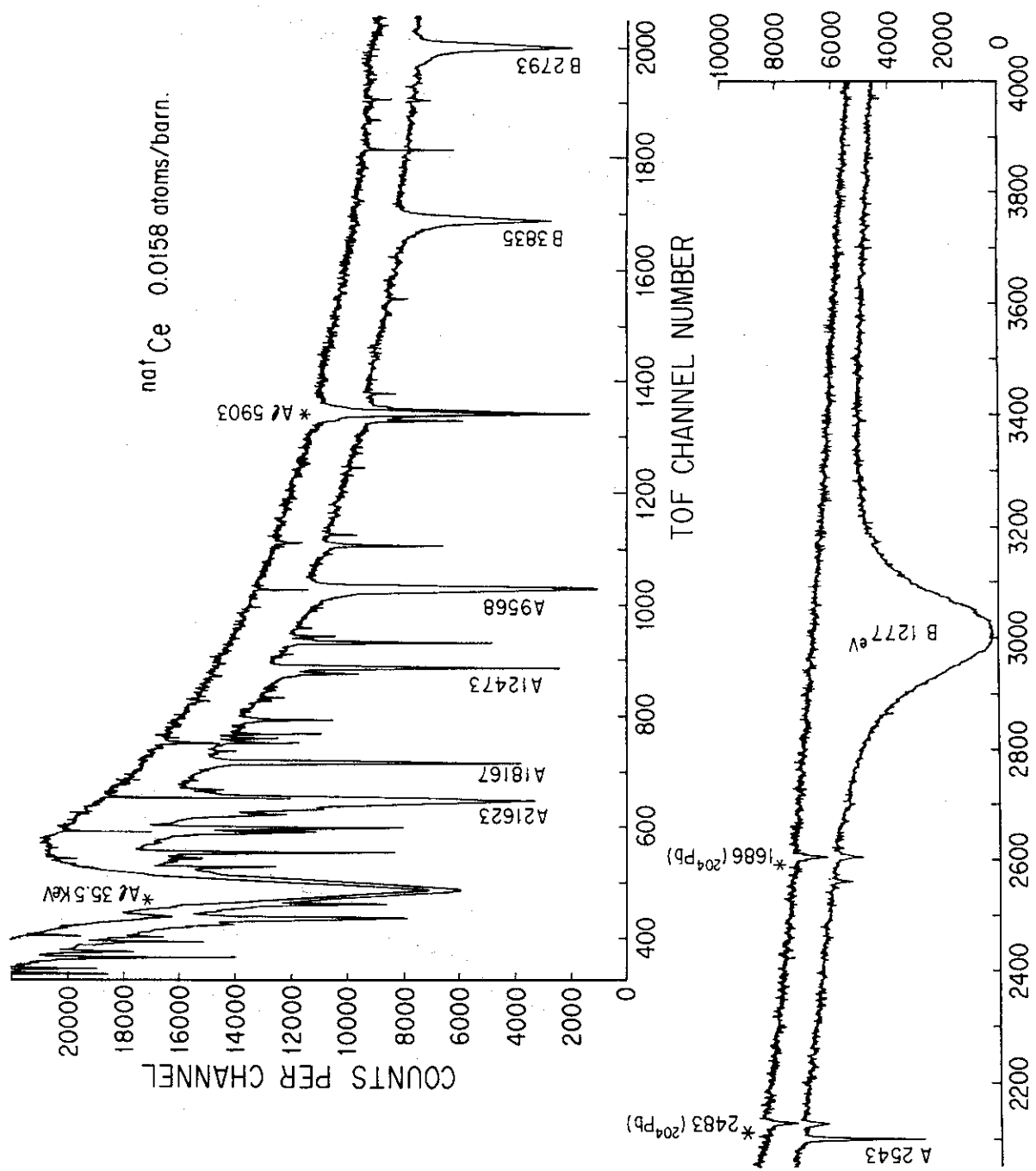


Fig.11 Raw data of neutron transmission measurements on natCe in the energy region from 1 keV to 100 keV. Sample thickness is 0.0158 Å/B, and channel width 31.25 ns.

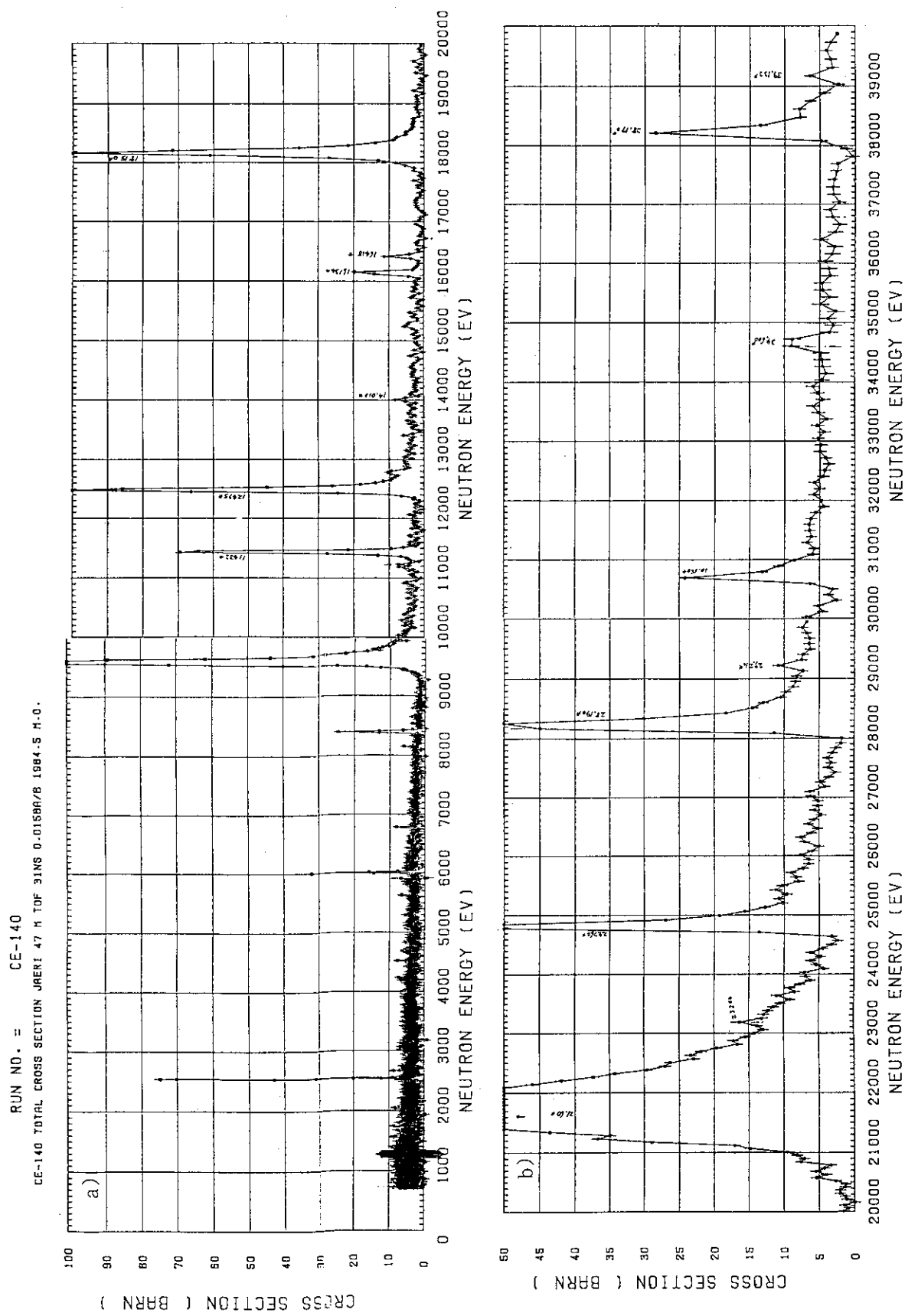
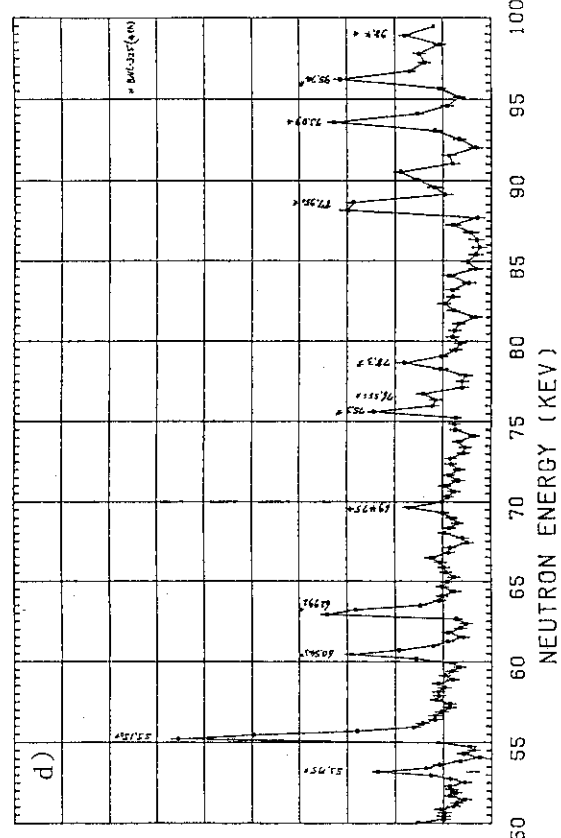
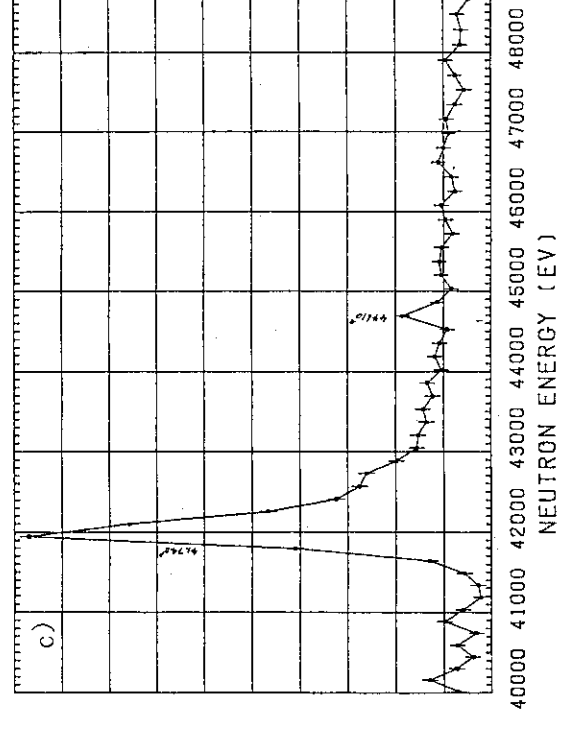


Fig.12 Total cross section of ^{140}Ce from 1 keV to 100 keV. A resonance at 21.6 keV has large width $T = 600$ eV.



RUN NO. = CE-142
 CE-142 TOTAL CROSS SECTION JAERI 47M TDF 31NS 0.0170A/B 1984.5 M.O.

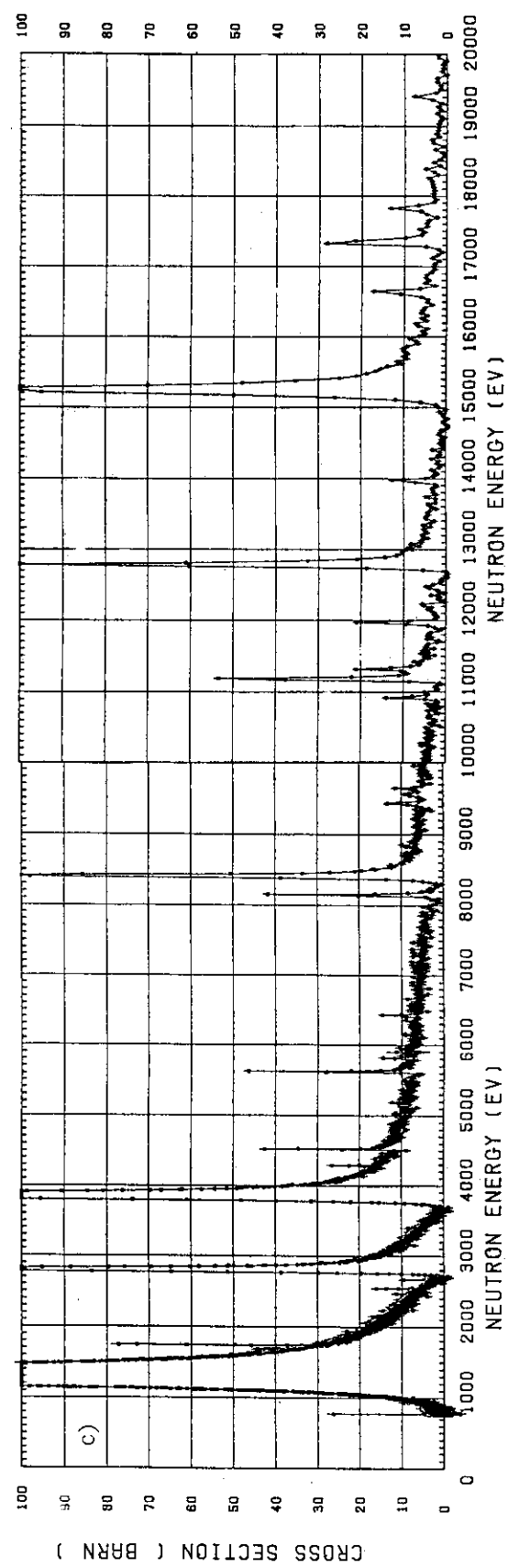
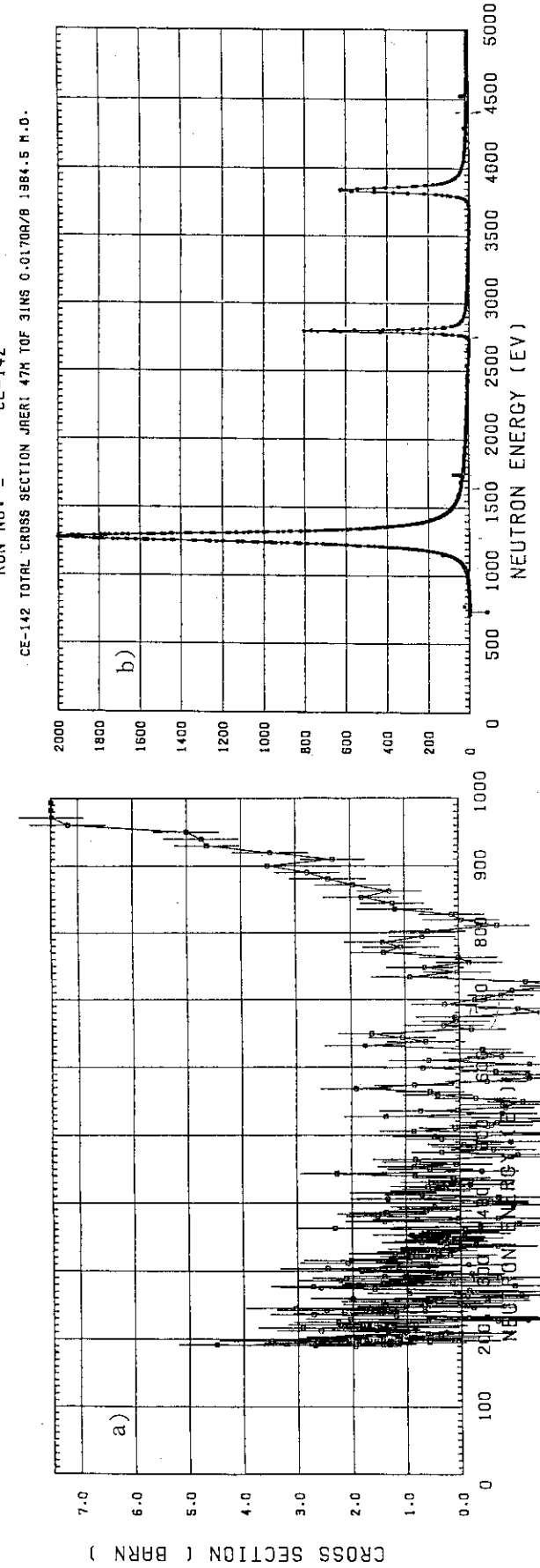
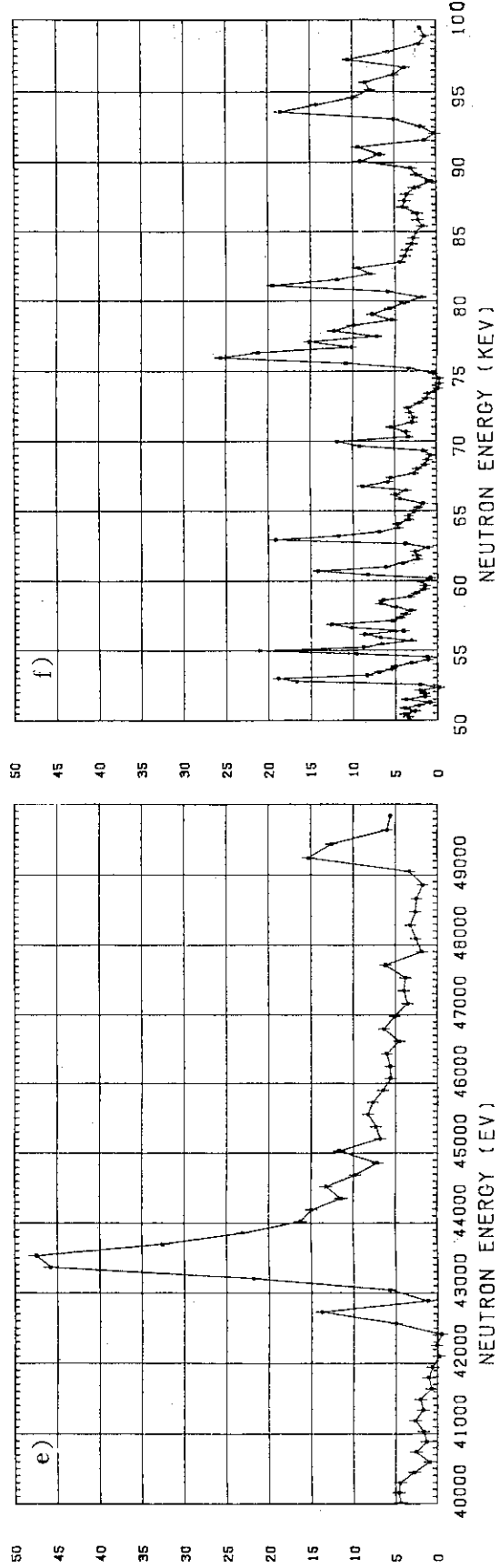
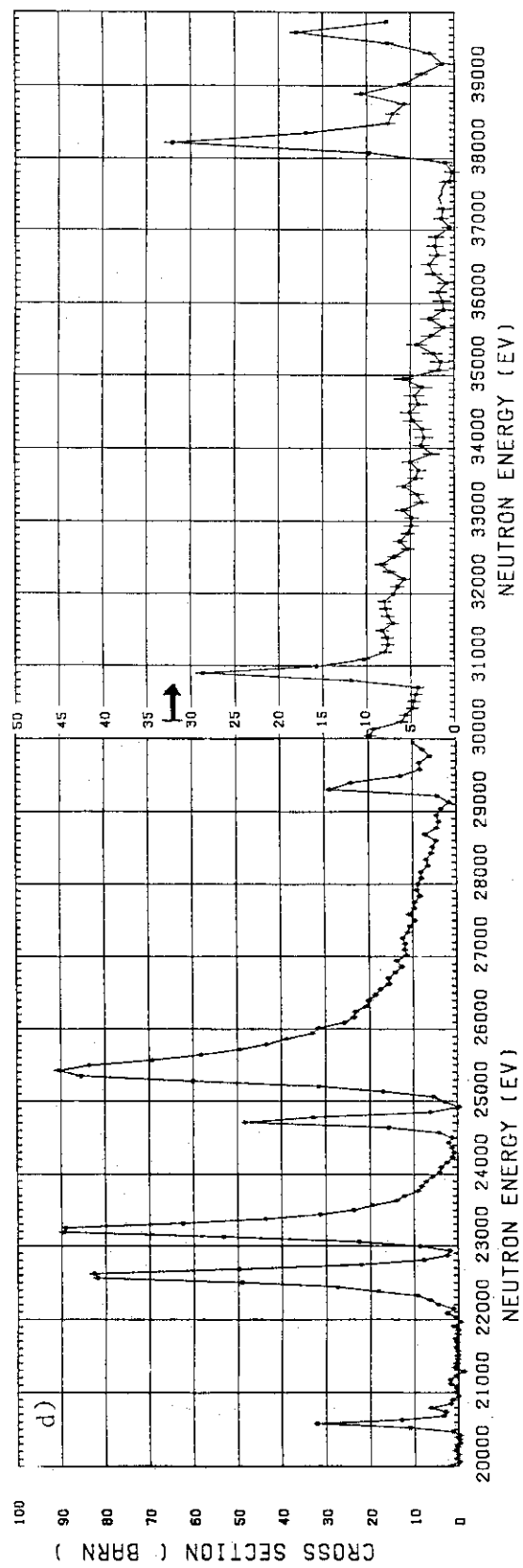


Fig.13 Total cross section of ^{142}Ce from 0.2 keV to 100 keV. The peak cross section of lowest 1.27 keV resonance is observed to be 2000 barn, and the potential-resonance interference minimum is observed at 600 ± 100 eV.

RUN NO. = CE-142
 CE-142 TOTAL CROSS SECTION 31.25NS 48.22M 0.0170A/B 1984.5



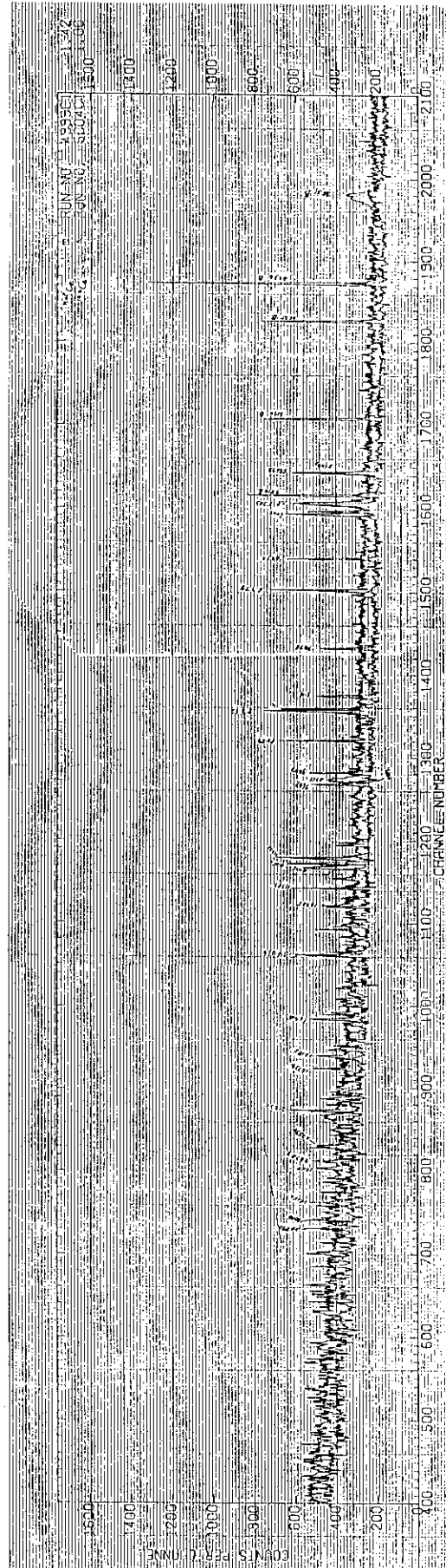


Fig.14 Capture raw data for ^{nat}Ce and ^{142}Ce samples observed by the liquid scintillator tank. Many probable p-wave resonances are observed.

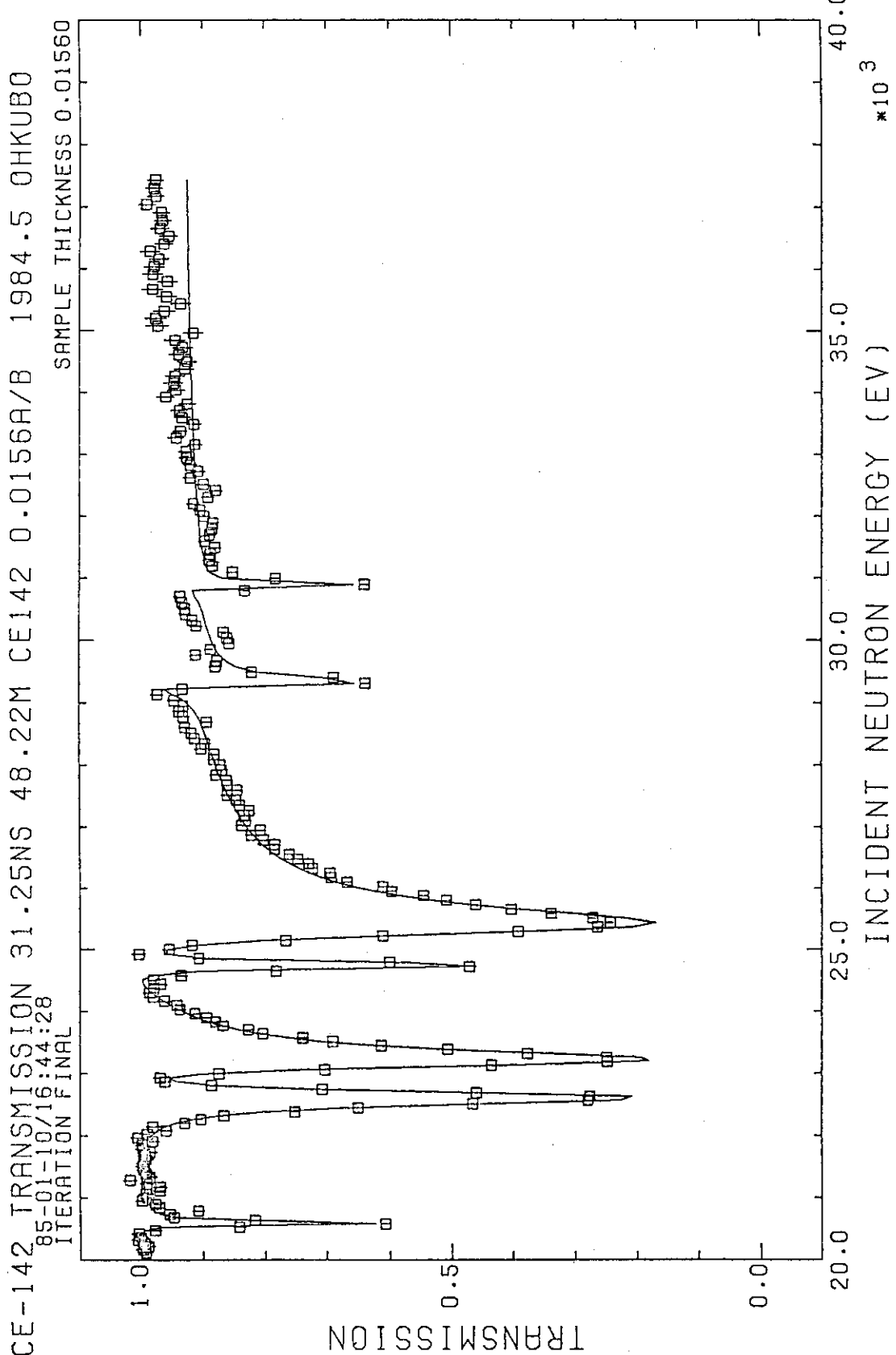


Fig.15 Transmission curve fitting by the SIOB code, for the resonances of ^{142}Ce from 20 to 37 keV.

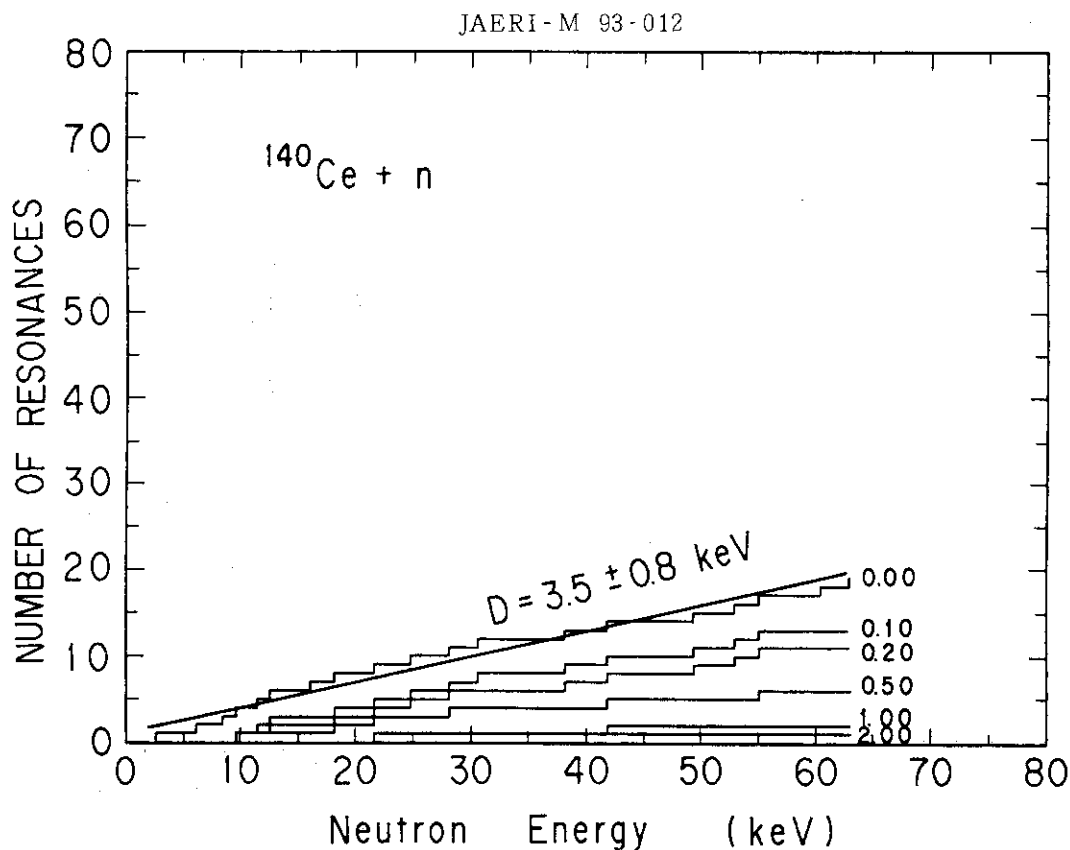


Fig.16 Cumulative number of levels vs. neutron energy for ^{140}Ce , where cut off in Γ_n^0 are made. Average level spacing is deduced to be 3.5 ± 0.8 keV.

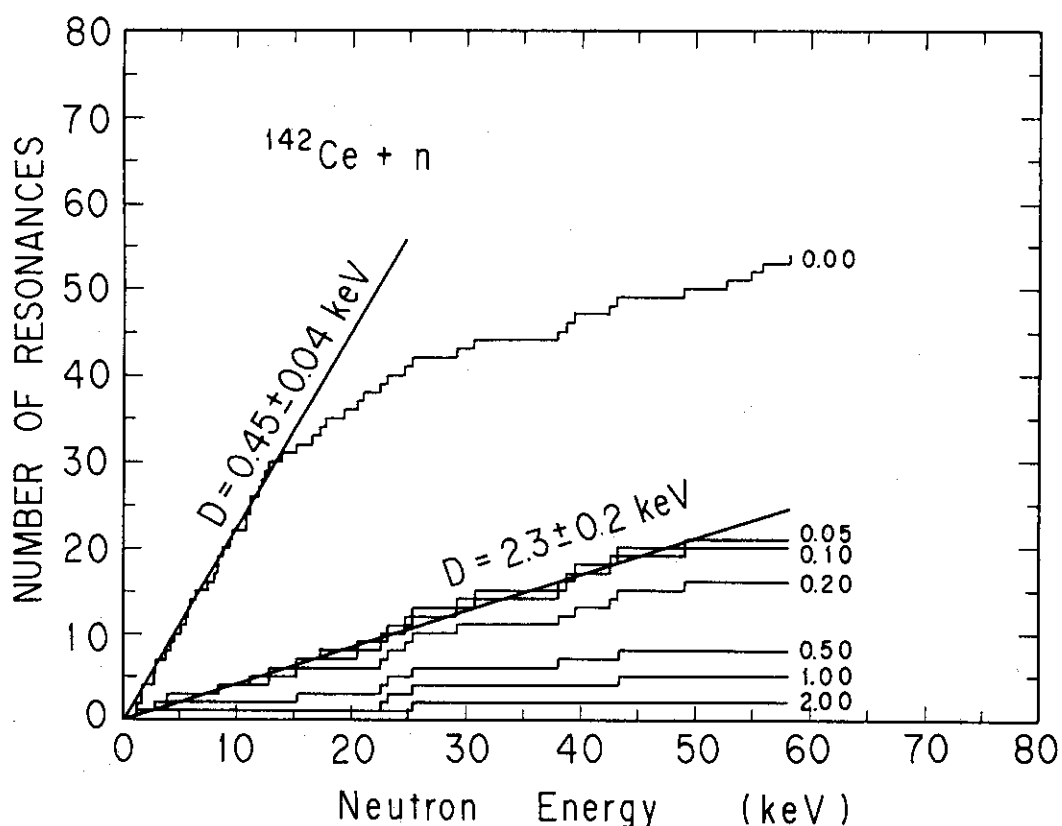


Fig.17 Cumulative number of levels vs. neutron energy for ^{142}Ce where cut off in Γ_n^0 are made. Average level spacing is deduced to be 2.3 ± 0.2 keV for s-wave levels, and to be 0.45 ± 0.1 keV with the inclusion of small probable p-wave levels.

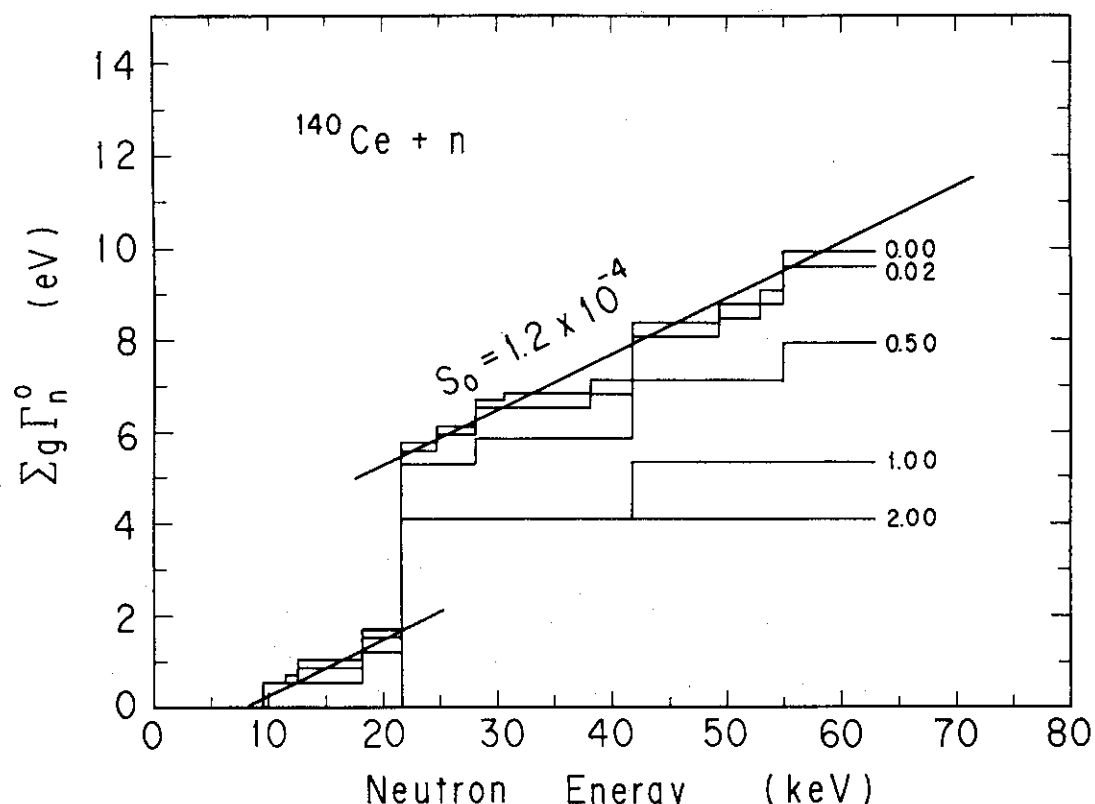


Fig.18 Cumulative values of Γ_n^0 for ^{140}Ce up to 55 keV. s_0 is estimated to be $(1.2 \pm 0.4) \times 10^{-4}$ if the contribution of 21.6 keV resonance is excluded, whereas s_0 is $(1.6 \pm 0.5) \times 10^{-4}$ if the contribution is included.

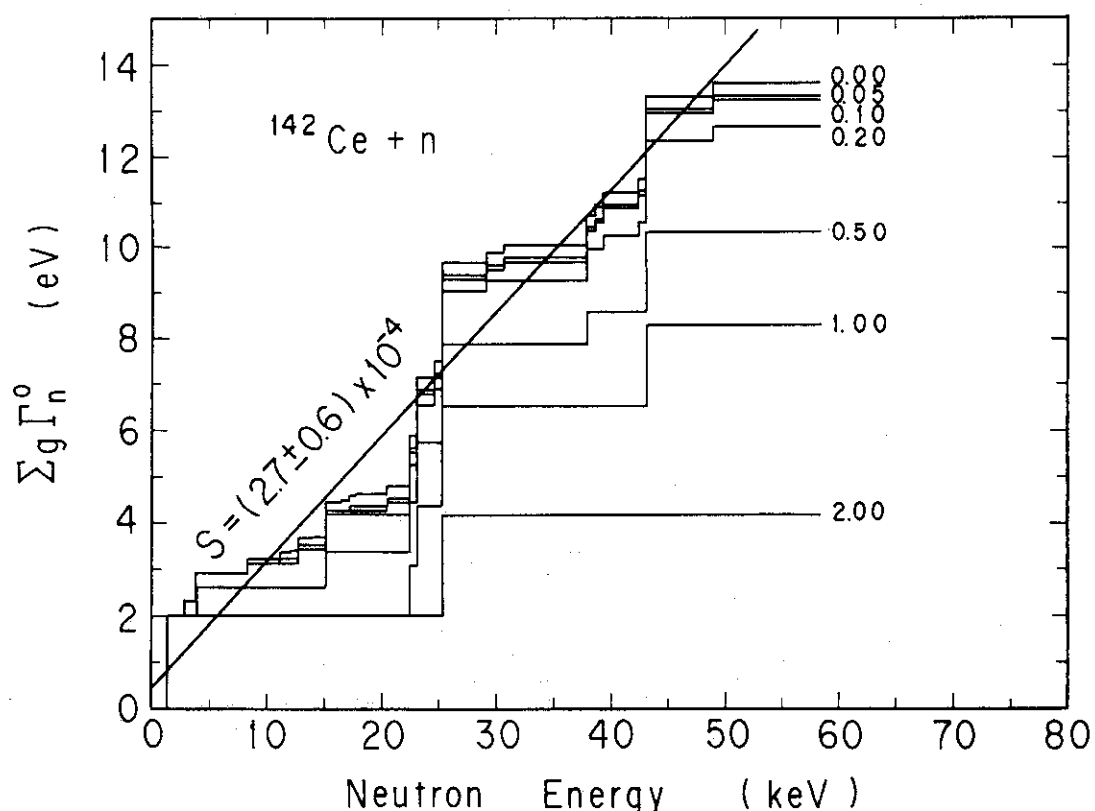


Fig.19 Cumulative values of Γ_n^0 for ^{142}Ce up to 55 keV. s_0 is estimated to be $(2.7 \pm 0.6) \times 10^{-4}$.

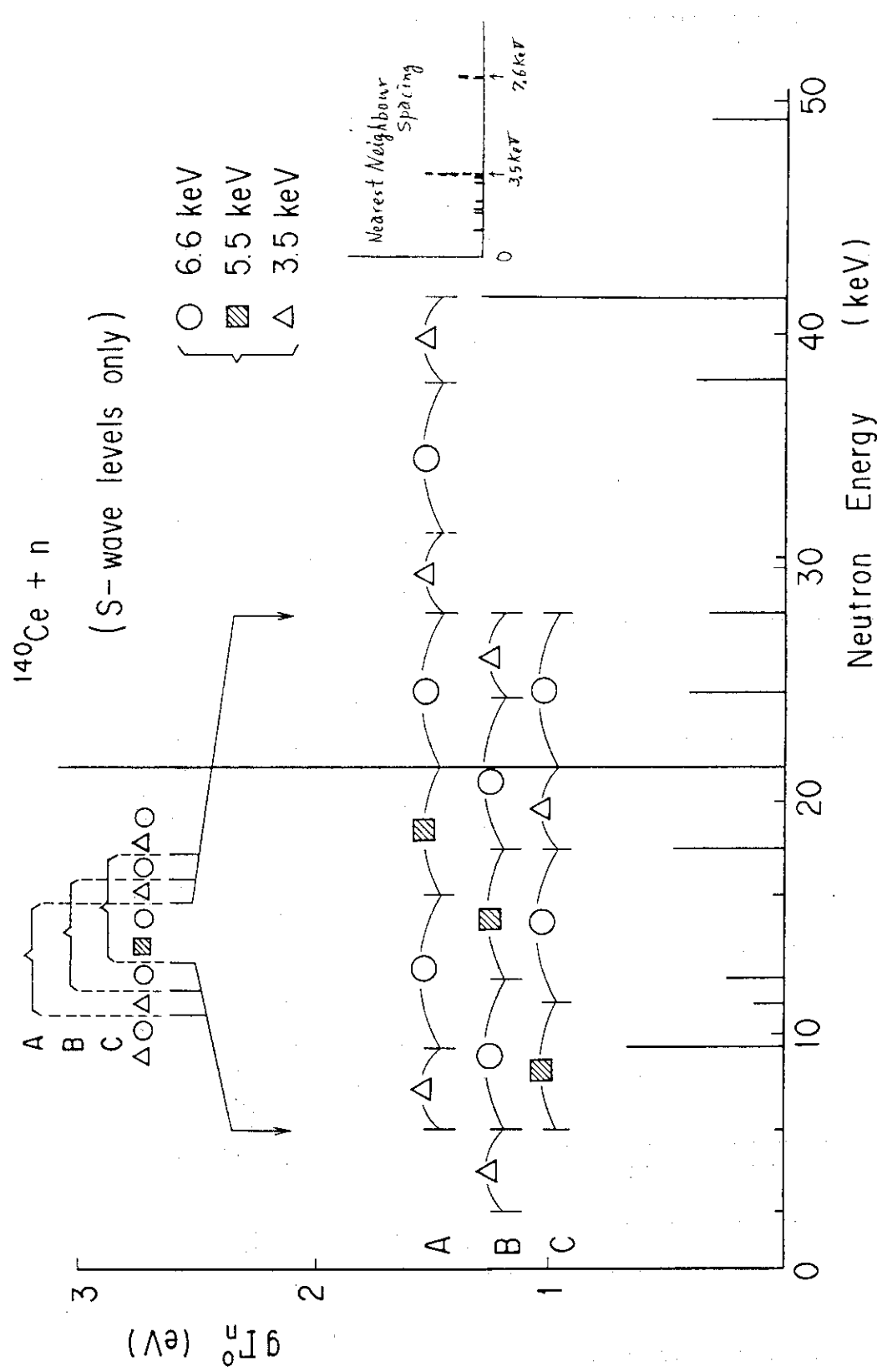


Fig. 20 Resonance level dispositions of ^{140}Ce below 50 keV. Level spacings of 3.5, 5.5 and 6.6 keV appear frequently among the levels. Many of the levels situate on the points combined by the three spacings. Between these spacings, integer ratios appear: $3.5/5.5 = 7/11$, and $5.5/6.6 = 5/6$. Series of $3.5 - 6.6 - 5.5 - 6.6 - 3.5$ or its fractions appear many times overlappingly. Moreover, integer ratios appear between the resonance energies: $21.60/9.57 = 9/4$, $21.60/18.06 = 6/5$, $21.60/24.76 = 7/8$, $21.60/28.19 = 10/13$.

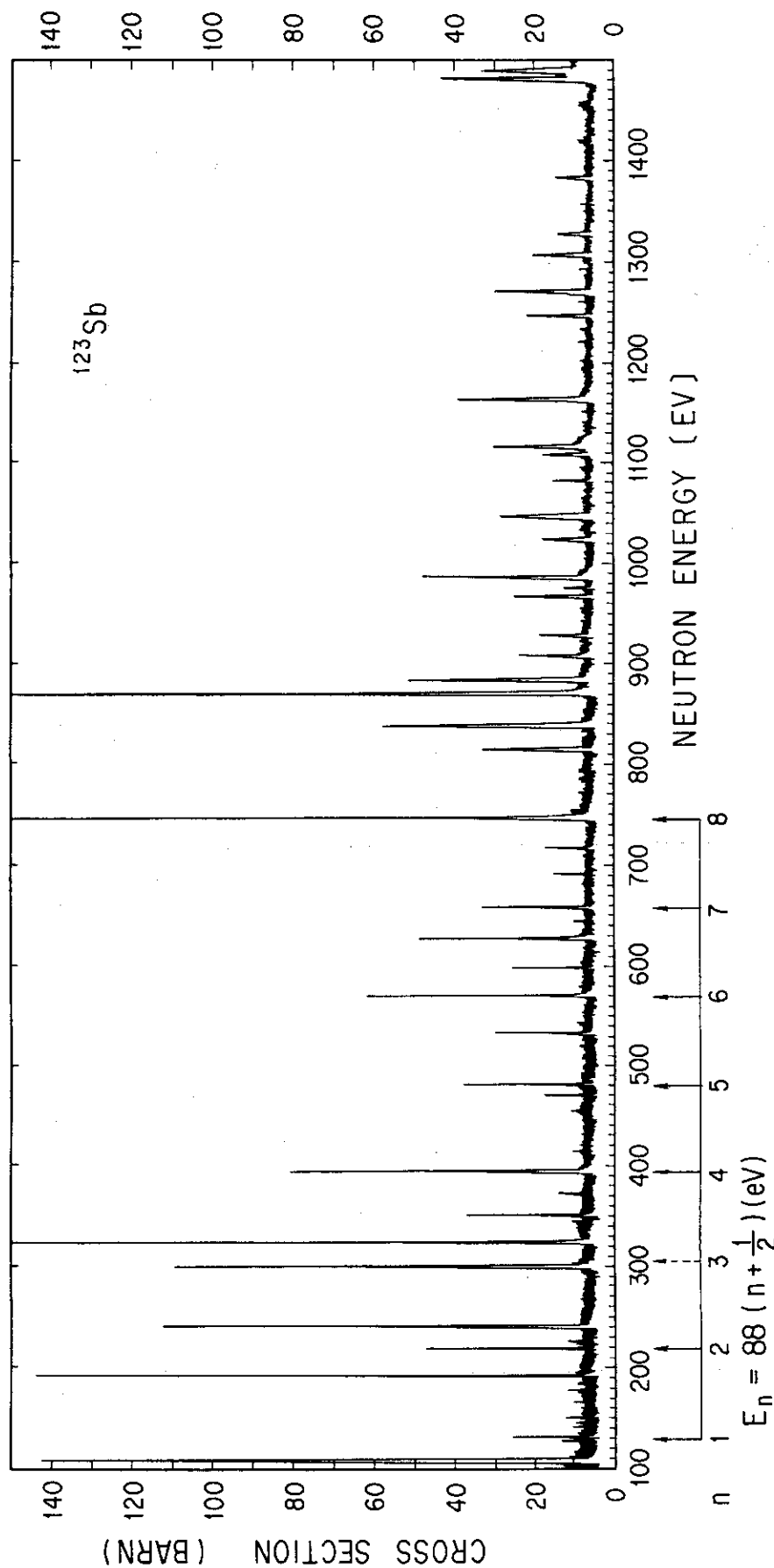


Fig.21 Total cross section of ^{123}Sb from 100 eV to 1500 eV, where a equidistant level series with energy at $E_n = 88 (n+1/2)$ ($n=1, 2, \dots, 8$) is seen.